PDF modeling for inhomogeneous turbulence with exact representation of rapid distortions

P. R. Van Slooten and S. B. Pope
Sibley School of Mechanical and Aerospace Engineering, Cornell University, Ithaca, New York 14853

(Received 30 August 1996; accepted 5 December 1996)

A model for inhomogeneous turbulence is constructed that provides an exact representation of rapidly distorted homogeneous turbulence (RDT). The fundamental quantity modeled is the joint PDF of the velocity and wave vector which is related to the unit wavenumber vector. This joint PDF provides a model equation for the evolution of the *directional spectrum*, the integral over the wavenumber magnitude of the velocity spectrum. At this level the rapid pressure–rate-of-strain correlation is closed yielding exact equations in RDT. For decaying turbulence, the return-to-isotropy terms are modeled by stochastic diffusion equations for the velocity and wave vector. A general model of this type is constructed along with four simplified versions. The decay models are combined with the RDT model to give complete models for homogeneous turbulence, which are tested for several flows. The homogeneous models are then extended in a general manner to inhomogeneous turbulence. © *1997 American Institute of Physics.* [S1070-6631(97)01404-9]

I. INTRODUCTION

A fundamental goal in turbulence modeling is the creation of robust and accurate models for the Reynolds stress equation. Although the present work is in the context of PDF methods, modeled Reynolds stress equations are still derived. The background for PDF methods is then best understood in the context of Reynolds stress models (RSM's).

For a wide range of inhomogeneous and homogeneous turbulent flows the rapid pressure–rate-of-strain correlation is a dominant term, which makes its modeling crucial to all RSM's. The standard modeling approach is based on the exact integral expressions derived by Chou[1] for the case of homogeneous turbulence. The integrals are not closed for RSM's, but are instead modeled as functions of the Reynolds stress anisotropy tensor. The slow or turbulent-turbulent interaction term requires the modeling of a second-order tensor, **B**, while for the rapid term a model of a fourth-order tensor, **M**, is required. Rotta[2] created the first model of this form by approximating the slow tensor as a linear function of the anisotropies. Other researchers have since formulated models for both tensors with varying levels of complexity. Some of the rapid models created are presented in the following references: Launder, Reece, and Rodi;[3] Shih and Lumley;[4] Haworth and Pope;[5] Fu, Launder, and Tselepidakis;[6] Speziale, Sarkar, and Gatski;[7] Johansson and Hallbäck;[8] and Ristorcelli, Lumley, and Abid;[9] while other slow models are presented in: Lumley and Newman;[10] Sarkar and Speziale;[11] and Chung and Kim.[12]

The general results of the rapid models have been mixed. For simple irrotational flows with small anisotropies, the latest models work very well, but for arbitrarily complex inhomogeneous flows RSM's have not performed up to expectations. This is particularly true for flows that contain rotational effects. In fact, recent analysis indicates that all RSM's are fundamentally flawed in certain rotational flows. Reynolds[13] demonstrated that the rapid rotation of anisotropic turbulence in RSM's has no effect on the invariants of the Reynolds stress anisotropy tensor, while the exact results from RDT (Cambon and Jacquin[14] and Mansour, Shih, and Reynolds[15]) indicate that the invariants decay. Reynolds and Kassinos[16] conclude that the Reynolds stress tensor forms an insufficient basis for modeling the rapid pressure–rate-of-strain correlation. In addition, Speziale, Abid, and Blaisdell[17] have shown that RSM's behave poorly when compared to linear stability analysis for complex rotational cases such as in elliptical flows. For homogeneous turbulence, linear stability theory is equivalent to RDT, so again the Reynolds stress closures fail for rapidly distorted rotating flows.

The study of RDT has a long history dating back to the original work of Prandtl[18] and Taylor.[19] Batchelor and Proudman[20] continued this work by deriving an exact expression for the Reynolds stresses in axisymmetric contraction and plane strain. Other references of note include: Townsend;[21] Lee and Reynolds;[22] Lee;[23] Lee, Kim, and Moin;[24] and Hunt and Carruthers.[25] Although the Reynolds stress equation for RDT includes the *unclosed* rapid pressure–rate-of-strain correlation, a closed and linear representation exists in Fourier space from which the exact solutions for the Reynolds stresses are derived. RSM's are often constructed to yield the correct *initial* response when *isotropic* turbulence is subjected to a particular rapid distortion, but the results for general flows in the RDT limit are typically unsatisfactory.

As a means to introduce improved modeling of the RDT limit Reynolds and Kassinos[16] and Kassinos and Reynolds[26] have gone beyond standard RSM approaches by including structural information of the turbulence. For RDT, they have added evolution equations for another second-order tensor, which they call the *structure dimensionality*. This allows increased functionality of the model for **M**, but introduces new closure problems in the equation for the dimensionality tensor. Additionally, a new model formulation for RDT based on an eddy axis tensor is presented. The results for this RDT model are very good, and an extension to non-RDT flows is presented in Kassinos and Reynolds.[27] Improving the extended model is a topic of their current research.[28]

The contribution of the present work is the development

of a general PDF model for inhomogeneous turbulence that maintains the exact solution for rapid distortions of homogeneous turbulence. Standard PDF methods for inert flows consist of models for the PDF of velocity (Pope[29] and Haworth and Pope[5]) or joint PDF of velocity and turbulent frequency (Pope and Chen[30] and Pope[31]), while in reacting flows composition is also included (Pope[29]). PDF methods have several advantages over traditional moment closures (Pope[29,32]). In particular, realizability is assured by construction so that a RSM is expressible by a PDF model only if it maintains realizability (Pope;[33] Durbin and Speziale;[34] and Wouters, Peeters, and Roekaerts[35]). Also, convection and reaction are treated exactly which are very important issues for inhomogeneous turbulence and reacting flows, respectively (Pope[29]). To achieve exact representation for rapid distortions, the standard velocity PDF models are extended by the inclusion of a stochastic vector, $\mathbf{e}^*$, called the wave vector. The added directional information results in a model for physical space variables that corresponds to the *directional spectrum* in Fourier (wavenumber) space. Thus, the model forms a bridge between Reynolds stress modeling and spectral modeling.

This work begins in Sec. II A with a brief introduction to the issues at the RSM level. Definitions and properties of spectral variables are presented in Sec. II B. A further introduction to the general theory of rapid distortions is presented in Sec. III A, while a wave space PDF formulation for RDT is constructed in Sec. III B. An equivalent PDF formulation for RDT in physical space is described in Sec. III C with a further examination of the correspondences between the stochastic and physical systems given in Sec. III D. The approaches utilized in Secs. III B, III C, and III D are an adaptation of the particle representation model for RDT presented by Kassinos and Reynolds[26] and are a Monte Carlo integration of the RDT governing equations. The new construction is designed to contain the formulation used in PDF methods which allows the extension of the method to non-RDT flows.

In Sec. IV A, the approach and motivations for the extension to general (i.e., non-RDT) homogeneous turbulence are examined. The idea is to construct a model for decaying turbulence which is then combined with the RDT model to yield a model for general homogeneous turbulence. In Sec. IV B, a general model for decaying turbulence along with four simplified models are derived and presented. The combined models are tested for several types of flows and the results discussed in Sec. IV C. The further extension of the homogeneous model to inhomogeneous turbulence is introduced in Sec. V, while a brief summary of the results and conclusions are given in Sec. VI.

II. BACKGROUND

A. Reynolds stress closures

The primary issues in turbulence modeling are addressed in homogeneous turbulent flows of Newtonian fluids with constant density, ρ, and kinematic viscosity, ν. The incompressible Navier-Stokes equations govern the evolution of the Eulerian velocity, $\mathbf{U}(\mathbf{x},t)$, which is also expressed in terms of its mean, $\langle \mathbf{U}(\mathbf{x},t)\rangle$, and fluctuation, $\mathbf{u}(\mathbf{x},t)$:

$$\mathbf{U}(\mathbf{x},t)=\langle \mathbf{U}(\mathbf{x},t)\rangle+\mathbf{u}(\mathbf{x},t). \tag{1}$$

For homogeneous turbulence the mean velocity is specified by a spatially uniform mean velocity gradient. The fluctuating velocity is described by continuity and conservation of momentum equations which are derived from the Navier-Stokes equations:

$$\frac{\partial u_i}{\partial x_i}=0, \tag{2a}$$

and

$$\frac{\partial u_i}{\partial t}+u_l\frac{\partial u_i}{\partial x_l}+u_l\frac{\partial \langle U_i\rangle}{\partial x_l}+\langle U_l\rangle\frac{\partial u_i}{\partial x_l}=-\frac{\partial P'}{\partial x_i}+\nu\frac{\partial^2 u_i}{\partial x_l\partial x_l}. \tag{2b}$$

The Reynolds stresses, $\langle u_i u_j\rangle$, are the primary variable of interest in turbulence modeling. Their evolution is derived from Eq. (2b) with the condition of statistical homogeneity applied:

$$\frac{d\langle u_i u_j\rangle}{dt}=\mathscr{P}_{ij}+\Pi_{ij}-\varepsilon_{ij}, \tag{3a}$$

where the symbolic terms are: production, $\mathscr{P}_{ij}$; pressure–rate-of-strain correlation, Π_{ij}; and dissipation, ε_{ij}. These terms are defined by

$$\mathscr{P}_{ij}\equiv-\langle u_i u_l\rangle\frac{\partial\langle U_j\rangle}{\partial x_l}-\langle u_l u_j\rangle\frac{\partial\langle U_i\rangle}{\partial x_l}, \tag{3b}$$

$$\Pi_{ij}\equiv 2\langle P' s_{ij}\rangle, \tag{3c}$$

and

$$\varepsilon_{ij}\equiv\nu\left\langle\frac{\partial u_i}{\partial x_k}\frac{\partial u_j}{\partial x_k}\right\rangle, \tag{3d}$$

where the fluctuating pressure, P', and the fluctuating rate-of-strain, $s_{ij}\equiv\frac{1}{2}(\partial u_i/\partial x_j+\partial u_j/\partial x_i)$, are used.

The Reynolds stresses are split into isotropic and anisotropic parts through the use of the turbulent kinetic energy, $k\equiv\frac{1}{2}\langle u_l u_l\rangle$, and the anisotropy of the Reynolds stresses:

$$b_{ij}\equiv\frac{\langle u_i u_j\rangle}{2k}-\tfrac{1}{3}\delta_{ij}. \tag{4}$$

For incompressible, homogeneous turbulence the Reynolds stress anisotropy equation is

$$\frac{db_{ij}}{dt}=\mathscr{P}_{ij}^{(b)}+\frac{1}{2k}\Pi_{ij}-\frac{\varepsilon}{k}(e_{ij}-b_{ij}), \tag{5a}$$

where

$$\mathscr{P}_{ij}^{(b)}\equiv\frac{1}{2k}[\mathscr{P}_{ij}-\mathscr{P}_{ll}(b_{ij}+\tfrac{1}{3}\delta_{ij})], \tag{5b}$$

and

$$e_{ij}\equiv\frac{\varepsilon_{ij}}{2\varepsilon}-\tfrac{1}{3}\delta_{ij}. \tag{5c}$$

In terms of a RSM, the production of anisotropy, $\mathscr{P}_{ij}^{(b)}$, is in closed form, while models are required for the pressure–rate-of-strain correlation and the dissipation tensor from which both the dissipation, $\varepsilon\equiv\frac{1}{2}\varepsilon_{ll}$, and the deviatoric dissipation, e_{ij}, are derived.

Chou[1] derived integral expressions for the pressure–rate-of-strain correlation in homogeneous turbulence from the exact solution of the Poisson equation for the fluctuating pressure:

$$\frac{\partial^2 P'}{\partial x_l \partial x_l} = \underbrace{-2\frac{\partial \langle U_l \rangle}{\partial x_m}\frac{\partial u_m}{\partial x_l}}_{\text{rapid}} \underbrace{-\frac{\partial u_l}{\partial x_m}\frac{\partial u_m}{\partial x_l}}_{\text{slow}} \tag{6}$$

Corresponding to the two source terms, the pressure–rate-of-strain correlation is split into rapid and slow parts, $\Pi_{ij} \equiv \Pi_{ij}^{(r)} + \Pi_{ij}^{(s)}$. The rapid correlation is expressed as a function of a fourth-order tensor, $\boldsymbol{M}$:

$$\Pi_{ij}^{(r)} = 4k\frac{\partial \langle U_l \rangle}{\partial x_k}(M_{ikjl} + M_{jkil}), \tag{7}$$

which is closed at the level of the two-point velocity correlation, $R_{ik}(\boldsymbol{r}) \equiv \langle u_i(\boldsymbol{x}) u_k(\boldsymbol{x}+\boldsymbol{r}) \rangle$:

$$M_{ikjl} \equiv -\frac{1}{8\pi k}\int \frac{1}{|\mathbf{r}|}\frac{\partial^2 R_{ik}(\boldsymbol{r})}{\partial r_j \partial r_l} d\mathbf{r}. \tag{8}$$

The slow correlation is expressed as a function of a second-order tensor, $\boldsymbol{B}$:

$$\Pi_{ij}^{(s)} = \varepsilon(B_{ij} + B_{ji}), \tag{9a}$$

which is closed at the level of the two-point triple velocity correlation, $C_{ikl}(\boldsymbol{r}) \equiv \langle u_i(\mathbf{x}) u_k(\mathbf{x}+\mathbf{r}) u_l(\mathbf{x}+\mathbf{r}) \rangle$:

$$B_{ij} \equiv -\frac{1}{4\pi\varepsilon}\int \frac{1}{|\mathbf{r}|}\frac{\partial^3 C_{ikl}(\boldsymbol{r})}{\partial r_j \partial r_k \partial r_l} d\mathbf{r}. \tag{9b}$$

The assumption of local isotropy at high Reynolds numbers yields an isotropic dissipation tensor. For lower Reynolds numbers, the slow pressure–rate-of-strain correlation and the deviatoric dissipation are combined to give the return-to-isotropy tensor, ϕ_{ij}:

$$\phi_{ij} \equiv -\frac{1}{\varepsilon}\Pi_{ij}^{(s)} + 2e_{ij}. \tag{10}$$

For the stress anisotropy equation, dissipation effects from the kinetic energy equation scale in a similar manner as the return-to-isotropy tensor, and they are both labeled as *slow* terms. The resulting Reynolds stress anisotropy equation is

$$\frac{db_{ij}}{dt} = \mathscr{P}_{ij}^{(b)} + \frac{1}{2k}\Pi_{ij}^{(r)} - \frac{\varepsilon}{2k}(\phi_{ij} - 2b_{ij}), \tag{11}$$

in which there are three terms that require modeling: the rapid pressure–rate-of-strain correlation; the dissipation; and the return-to-isotropy tensor.

For a rotating reference frame, the Reynolds stress equations are altered in two ways:

(i) the Coriolis force adds kinematic terms similar to the production;
(ii) the rapid pressure–rate-of-strain correlation includes the frame rotation rate tensor.

The frame rotation is expressed through either the frame rotation rate tensor, $\boldsymbol{\Omega}^f$, or the angular velocity of the frame, $\overline{\boldsymbol{\Omega}^f}$, which are related via $\Omega_{ij}^f = \overline{\Omega}_m^f \epsilon_{imj}$.

B. Wavenumber space variables

In the later development of stochastic PDF models it is crucial to demonstrate the level of correspondence between the stochastic and the physical systems. This correspondence occurs in wavenumber space, and certain spectral variables are required to relate the results to the Reynolds stresses. The velocity spectrum is defined as the Fourier transform of the two-point velocity correlation:

$$\Phi_{ij}(\boldsymbol{\kappa}) \equiv \left(\frac{1}{2\pi}\right)^3 \int R_{ij}(\mathbf{r}) e^{-\imath \boldsymbol{\kappa}\cdot\mathbf{r}} d\mathbf{r}. \tag{12}$$

The integral of the symmetric part of this tensor, $\Phi_{ij}^s \equiv \frac{1}{2}(\Phi_{ij} + \Phi_{ji})$, over the magnitude of the wavenumber vector, $\kappa \equiv |\boldsymbol{\kappa}|$, defines the *directional spectrum*:

$$\Gamma_{ij}(\mathbf{e}) \equiv \int_0^\infty \kappa^2 \Phi_{ij}^s(\kappa\mathbf{e}) d\kappa, \tag{13}$$

where $\mathbf{e} \equiv \boldsymbol{\kappa}/\kappa$ is the unit wavenumber vector. The directional spectrum is symmetric by definition and real due to conjugate symmetry. Related to the directional spectrum is the *directional energy spectrum*:

$$\Gamma(\mathbf{e}) \equiv \tfrac{1}{2}\Gamma_{ll}(\mathbf{e}). \tag{14}$$

The spectral variables are related to the Reynolds stresses and the turbulent kinetic energy through the inverse Fourier transform:

$$\langle u_i u_j \rangle = \int \Phi_{ij}(\boldsymbol{\kappa}) d\boldsymbol{\kappa} = \int \Gamma_{ij}(\mathbf{e}) dS(\mathbf{e}), \tag{15a}$$

and

$$k = \int \Gamma(\mathbf{e}) dS(\mathbf{e}), \tag{15b}$$

where $dS(\mathbf{e})$ is the differential element on the surface of the unit sphere. These relationships provide valuable physical interpretations of the spectral variables. The velocity spectrum is the Reynolds stress density in wavenumber space, while the directional spectrum and the directional energy spectrum are the densities on the unit sphere in wavenumber space of the Reynolds stresses and turbulent kinetic energy, respectively.

The form of the spectral variables in isotropic turbulence is a useful property. For the velocity spectrum the isotropic form is well known (Batchelor[36]):

$$\Phi_{ij}(\boldsymbol{\kappa}) = \frac{E(\kappa)}{4\pi\kappa^2}\left(\delta_{ij} - \frac{\kappa_i \kappa_j}{\kappa^2}\right), \tag{16}$$

where $E(\kappa)$ is the energy spectrum,

$$E(\kappa) \equiv \int \frac{1}{2}\Phi_{ll}(\kappa\mathbf{e})\kappa^2 dS(\mathbf{e}). \tag{17}$$

The isotropic form of the directional spectrum is independent of the energy spectrum:

$$\Gamma_{ij}(\mathbf{e}) = \frac{k}{4\pi}(\delta_{ij} - e_i e_j), \tag{18}$$

while the directional energy spectrum is uniform over the unit sphere:

$$\Gamma(\mathbf{e}) = \frac{k}{4\pi}. \tag{19}$$

The spectral variables are also related to the fourth-order tensor in the rapid pressure–rate-of-strain correlation:

$$M_{ikjl} = \frac{1}{2k}\int \frac{\kappa_j \kappa_l}{\kappa^2}\Phi_{ik}(\boldsymbol{\kappa})\, d\boldsymbol{\kappa} = \frac{1}{2k}\int e_j e_l \Gamma_{ik}(\mathbf{e})\, dS(\mathbf{e}), \tag{20}$$

so that knowledge of either the velocity or directional spectrum is sufficient to *close* the rapid pressure–rate-of-strain correlation for *all* homogeneous turbulent flows. Therefore, modeling approaches that are based on either spectrum can provide improved results over RSM's.

III. RAPID DISTORTION THEORY

A. General theory

In turbulence modeling the quantities of interest (i.e., Reynolds stresses) are dominated by the large, energy containing scales of the flow. For these scales, RDT applies when the mean distortion imposes a time scale, $S^{-1} \equiv \|\nabla \langle \mathbf{U} \rangle\|^{-1}$, on the flow that is much smaller than that of the large scales, $\tau \equiv k/\varepsilon$. This condition is expressed through a constraint on the normalized shear- (strain- or rotation-) rate parameter:

$$\left(\frac{Sk}{\varepsilon}\right) \gg 1. \tag{21}$$

The continuity equation, Eq. (2a), is unchanged by this scaling, but the turbulent convection and the viscous terms in Eq. (2b) and the slow pressure term in Eq. (6) are negligible. The momentum and Poisson pressure equations are then linear in the fluctuating velocity:

$$\frac{\partial u_i}{\partial t} + u_l \frac{\partial \langle U_i \rangle}{\partial x_l} + \langle U_l \rangle \frac{\partial u_i}{\partial x_l} = -\frac{\partial P'}{\partial x_i}, \tag{22a}$$

and

$$\frac{\partial^2 P'}{\partial x_l \partial x_l} = -2\frac{\partial \langle U_l \rangle}{\partial x_m}\frac{\partial u_m}{\partial x_l}. \tag{22b}$$

The Reynolds stress equation, Eq. (3a), and the anisotropy equation, Eq. (5a), are simplified by the elimination of the slow pressure–rate-of-strain correlation and the dissipation tensor:

$$\frac{d\langle u_i u_j \rangle}{dt} = \mathscr{P}_{ij} + \Pi_{ij}^{(r)}, \tag{23a}$$

and

$$\frac{db_{ij}}{dt} = \mathscr{P}_{ij}^{(b)} + \frac{1}{2k}\Pi_{ij}^{(r)}. \tag{23b}$$

For a single Fourier mode a general solution of Eq. (22) exists of the form:

$$\boldsymbol{u}(\boldsymbol{x},t) = \hat{\boldsymbol{u}}(t) e^{\imath \hat{\boldsymbol{\kappa}}(t)\cdot \boldsymbol{x}}, \tag{24}$$

where $\hat{\boldsymbol{u}}(t)$ is the Fourier velocity mode and $\hat{\boldsymbol{\kappa}}(t)$ is a time varying wavenumber. These variables evolve via

$$\frac{d\hat{u}_i}{dt} = -\frac{\partial \langle U_m \rangle}{\partial x_n}\hat{u}_n(\delta_{im} - 2\hat{e}_i\hat{e}_m), \tag{25a}$$

$$\frac{d\hat{\kappa}_i}{dt} = -\frac{\partial \langle U_m \rangle}{\partial x_i}\hat{\kappa}_m, \tag{25b}$$

and

$$\frac{d\hat{e}_i}{dt} = -\frac{\partial \langle U_m \rangle}{\partial x_n}\hat{e}_m(\delta_{in} - \hat{e}_i\hat{e}_n), \tag{25c}$$

where the evolution of the time varying unit wavenumber vector, $\hat{\boldsymbol{e}}(t) \equiv \hat{\boldsymbol{\kappa}}(t)/|\hat{\boldsymbol{\kappa}}(t)|$, is also given. The solution maintains continuity through

$$\hat{\boldsymbol{u}}(t)\cdot\hat{\boldsymbol{\kappa}}(t) = \hat{\boldsymbol{u}}(t)\cdot\hat{\boldsymbol{e}}(t) = 0. \tag{26}$$

The time varying wavenumbers are commonly viewed as a deforming space (Rogallo[37]), but interpreting them as a Lagrangian system of particles evolving in a fixed wave space is equivalent. This viewpoint provides a clearer picture of the modeling in this work.

The velocity spectrum is defined in a fixed wave space and is related to Fourier velocity modes in this fixed wave space. These modes, $\hat{\boldsymbol{a}}$, are defined in the standard manner by a Fourier series expansion of an assumed periodic velocity field with period L, which results in discrete wavenumbers, ℓ. The definitions of the two-point velocity correlation and the velocity spectrum are then used to give:

$$\Phi_{ij}(\boldsymbol{\kappa}) = \lim_{L\to\infty}\left(\frac{L}{2\pi}\right)^3 \sum_{\ell} \langle (\hat{\boldsymbol{a}}_i(\ell))^* \hat{\boldsymbol{a}}_j(\ell)\rangle \delta(\boldsymbol{\kappa} - \ell), \tag{27}$$

where the complex conjugate operator, $()^*$, is used, and a delta operator is defined to give a relationship between the discrete and continuous wavenumbers:

$$\delta(\boldsymbol{\kappa} - \ell) = \begin{cases} 1 & \boldsymbol{\kappa} = \ell, \\ 0 & \text{otherwise.} \end{cases} \tag{28}$$

From Eqs. (25) and (27), the RDT equation for the velocity spectrum is derived through the use of the standard Lagrangian to Eulerian transformation (see also Townsend[21] and Craya[38] for alternative derivations):

$$\frac{\partial \Phi_{ij}}{\partial t} = \kappa_m \frac{\partial \langle U_m \rangle}{\partial x_n}\frac{\partial \Phi_{ij}}{\partial \kappa_n} - \frac{\partial \langle U_j \rangle}{\partial x_m}\Phi_{im} - \frac{\partial \langle U_i \rangle}{\partial x_m}\Phi_{mj} + 2\frac{\partial \langle U_n \rangle}{\partial x_m}\left[\frac{\kappa_i \kappa_n}{\kappa^2}\Phi_{mj} + \frac{\kappa_j \kappa_n}{\kappa^2}\Phi_{im}\right]. \tag{29}$$

Integrating the symmetric part over the wavenumber magnitude yields the RDT equation for the directional spectrum:

$$\frac{\partial \Gamma_{ij}}{\partial t} = e_m(\delta_{rn} - e_r e_n)\frac{\partial \langle U_m \rangle}{\partial x_r}\frac{\partial \Gamma_{ij}}{\partial e_n} - 3 e_m e_r \frac{\partial \langle U_m \rangle}{\partial x_r}\Gamma_{ij} - \frac{\partial \langle U_j \rangle}{\partial x_m}\Gamma_{im} - \frac{\partial \langle U_i \rangle}{\partial x_m}\Gamma_{jm} + 2\frac{\partial \langle U_n \rangle}{\partial x_m}[e_i e_n \Gamma_{jm} + e_j e_n \Gamma_{im}]. \tag{30}$$

Both the velocity and directional spectra evolve via *closed* equations in the RDT limit under consideration. Also, the directional spectrum is a compact description of the flow in that no further simplification from it maintains a closed governing equation for RDT.

B. PDF formulation for RDT in Fourier space

In this work, PDF methods are viewed as modeling the exact and generally unclosed one-point, one-time PDF equations that are derived from the Navier-Stokes equations. The model PDF equation is constructed so that it is equivalent to the PDF equation for a simple stochastic system which is easily simulated via Monte Carlo techniques. In this section and the two following sections the particle representation model by Kassinos and Reynolds[26] is adapted for PDF methods. From this new construction the method is extendible to non-RDT flows. In addition, the construction illustrates differences between these PDF methods and standard PDF methods.

From the previous section the solution for a single Fourier mode in the RDT limit consists of ordinary differential equations for $\hat{\boldsymbol{\kappa}}$ and $\hat{\boldsymbol{u}}$. The equations for RDT are closed at the directional spectrum level for which it is sufficient to consider the unit wavenumber vector, $\hat{\boldsymbol{e}}$, in place of the full vector. For general initial velocity fields, the PDF formulation of the problem is constructed by setting the unit wavenumbers and velocity modes to be the random variables, $\hat{\boldsymbol{e}}^*$ and $\hat{\boldsymbol{u}}^*$, respectively. These stochastic variables evolve by the deterministic RDT equations, Eq. (25). The fundamental variable is then the joint PDF of unit wavenumber and velocity mode, $\hat{f}(\boldsymbol{\eta},\boldsymbol{v})$, where $(\boldsymbol{\eta},\boldsymbol{v})$ are the state space variables for $(\hat{\boldsymbol{e}}^*,\hat{\boldsymbol{u}}^*)$. The joint PDF equation as derived via standard approaches:

$$\frac{\partial \hat{f}}{\partial t} = \frac{\partial \langle U_r \rangle}{\partial x_s}\frac{\partial}{\partial \eta_i}\left[\eta_r\left(\delta_{is} - \frac{\eta_i \eta_s}{\eta^2}\right)\hat{f}\right] + \frac{\partial \langle U_r \rangle}{\partial x_s}\frac{\partial}{\partial v_i}\left[v_s\left(\delta_{ir} - 2\frac{\eta_i \eta_r}{\eta^2}\right)\hat{f}\right], \tag{31}$$

is an exact representation of the Navier-Stokes equations in the RDT limit. Therefore, a Monte Carlo simulation based on the stochastic variables, $\hat{\boldsymbol{e}}^*$ and $\hat{\boldsymbol{u}}^*$, is an exact Monte Carlo integration of the RDT equations.

The PDF approach for RDT in Fourier space is completed by the specification of an initial distribution of $\hat{\boldsymbol{e}}^*$ and $\hat{\boldsymbol{u}}^*$, while the velocity field requires the distribution of the stochastic wavenumber vector, $\hat{\boldsymbol{\kappa}}^*$. The velocity field that corresponds to N realizations of $\hat{\boldsymbol{\kappa}}^*$ and $\hat{\boldsymbol{u}}^*$ is equivalent to the sum of $2N$ modes:

$$\boldsymbol{u}(\boldsymbol{x}) = \sum_{n=-N}^{N} \hat{\boldsymbol{u}}^{(n)} e^{\imath \hat{\boldsymbol{\kappa}}^{(n)} \cdot \boldsymbol{x}}, \tag{32a}$$

where conjugate symmetry is maintained by

$$\hat{\boldsymbol{u}}^{(-n)} \equiv (\hat{\boldsymbol{u}}^{(n)})^* \quad \text{and} \quad \hat{\boldsymbol{\kappa}}^{(-n)} \equiv -\hat{\boldsymbol{\kappa}}^{(n)}, \quad \text{for } n = 1,N. \tag{32b}$$

In Appendix A, a method is developed for specifying the stochastic variables in a manner that results in a random homogeneous vector field with a prescribed spectrum. By comparison of Eqs. (32a) and (A11), a proper initial velocity field is generated, if

$$\hat{\boldsymbol{u}}^{(n)} = \frac{1}{\sqrt{2N}}\hat{\boldsymbol{Z}}^{(n)}, \tag{33a}$$

and

$$\hat{\boldsymbol{\kappa}}^{(n)} = \boldsymbol{\kappa}^{(n)}, \tag{33b}$$

where $\hat{\boldsymbol{Z}}^{(n)}$ is a zero-mean random vector whose covariance matrix is determined by the spectrum, Eq. (A12), and $\boldsymbol{\kappa}^{(n)}$ is a random vector with a distribution defined in Eq. (A4).

C. PDF formulation for RDT in physical space

The previous section constructed a PDF method for RDT using Fourier space variables. To extend this method for inhomogeneous turbulent flows, it is necessary to construct a method that is based on physical space variables. A stochastic system consisting of the velocity, $\mathbf{u}^*$, and a unit vector, $\mathbf{e}^*$, is written:

$$du_i^* = -\frac{\partial \langle U_r \rangle}{\partial x_s} u_s^*(\delta_{ir} - 2e_i^* e_r^*)dt, \tag{34a}$$

and

$$de_i^* = -\frac{\partial \langle U_r \rangle}{\partial x_s} e_r^*(\delta_{is} - e_i^* e_s^*)dt. \tag{34b}$$

These equations are identical to the evolution equations for the Fourier amplitude of velocity and the unit wavenumber, Eq. (25), which is the justification for labeling $\mathbf{e}^*$ the wave vector. Therefore, the one-point, one-time joint PDF of velocity and wave vector, $f^*(\mathbf{V},\boldsymbol{\eta})$, corresponds identically to $\hat{f}(\boldsymbol{v},\boldsymbol{\eta})$ since they evolve by the same equation:

$$\frac{\partial f^*}{\partial t} = \frac{\partial \langle U_r \rangle}{\partial x_s}\frac{\partial}{\partial \eta_i}\left[\eta_r\left(\delta_{is} - \frac{\eta_i \eta_s}{\eta^2}\right)f^*\right] + \frac{\partial \langle U_r \rangle}{\partial x_s}\frac{\partial}{\partial V_i}\left[V_s\left(\delta_{ir} - 2\frac{\eta_i \eta_r}{\eta^2}\right)f^*\right]. \tag{35}$$

Again, the stochastic system is an exact Monte Carlo integration for RDT, and is called the **u-e** RDT Model. The evolution of the stochastic system defined here, $(\mathbf{u}^*,\mathbf{e}^*)$, is analogous to the system from Kassinos and Reynolds,[26] $(\mathbf{v},\mathbf{n})$, where $\mathbf{v}$ is the velocity and $\mathbf{n}$ is the unit gradient vector.

The specification of a stochastic velocity evolution by the velocity Fourier mode equation requires justification which is demonstrated by the correspondence between the Reynolds stresses of the stochastic and physical systems. First, correspondence is established between the spectrum variables of RDT and the stochastic model through a stochastic tensor:

$$\Lambda_{ij}^*(\boldsymbol{\eta}) \equiv \int V_i V_j f^*(\mathbf{V},\boldsymbol{\eta}) d\mathbf{V} = \langle u_i^* u_j^* | \mathbf{e}^* = \boldsymbol{\eta} \rangle f_e^*(\boldsymbol{\eta}), \tag{36}$$

where the marginal PDF of the wave vector, $f_e^*(\boldsymbol{\eta})$, and the stochastic Reynolds stresses conditional on the wave vector (Kassinos and Reynolds[26]) are introduced. The evolution equation for the new tensor is found by integrating the joint PDF equation:

$$\begin{aligned}\frac{\partial \Lambda_{ij}^*}{\partial t} = {} & \eta_m \left(\delta_{rn} - \frac{\eta_r \eta_n}{\eta_t \eta_t} \right) \frac{\partial \langle U_m \rangle}{\partial x_r} \frac{\partial \Lambda_{ij}^*}{\partial \eta_n} \\ & - 3 \frac{\eta_m \eta_r}{\eta_t \eta_t} \frac{\partial \langle U_m \rangle}{\partial x_r} \Lambda_{ij}^* - \frac{\partial \langle U_j \rangle}{\partial x_m} \Lambda_{im}^* \\ & - \frac{\partial \langle U_i \rangle}{\partial x_m} \Lambda_{jm}^* + 2 \frac{\partial \langle U_n \rangle}{\partial x_m} \left[\frac{\eta_i \eta_n}{\eta_t \eta_t} \Lambda_{jm}^* + \frac{\eta_i \eta_n}{\eta_t \eta_t} \Lambda_{im}^* \right]. \end{aligned} \tag{37}$$

By comparison with Eq. (30) the new stochastic tensor is shown to evolve in the exact manner as the directional spectrum. Thus, it is the stochastic model for the directional spectrum (Kassinos and Reynolds[26]):

$$\Lambda_{ij}^*(\boldsymbol{\eta}) \leftrightarrow \Gamma_{ij}(\mathbf{e}). \tag{38}$$

The spectral correspondence is combined with the relationship between the Reynolds stresses and the directional spectrum, Eq. (15a), to demonstrate the correspondence between the Reynolds stresses from the physical and stochastic systems:

$$\langle u_i u_j \rangle = \int \Gamma_{ij}(\mathbf{e}) dS(\mathbf{e}) \leftrightarrow \int \Lambda_{ij}^*(\boldsymbol{\eta}) d\boldsymbol{\eta} = \langle u_i^* u_j^* \rangle. \tag{39}$$

Therefore, the equation for the Fourier mode of the velocity is an appropriate model for the stochastic velocity.

Both PDF methods based on this RDT approach and standard PDF methods provide a model for the rapid pressure term in the evolution equation for the PDF of velocity. However, standard PDF methods are constructed to correspond to the Reynolds stresses and RSM's, while the new methods correspond to the directional spectrum.

D. Correspondence to Reynolds stress and structure based models

With a PDF model based on the velocity and the wave vector, the evolution of the statistical quantities such as the Reynolds stresses are specified. The model Reynolds stress equation is derived from the stochastic evolution equation for the velocity:

$$\begin{aligned}\frac{d\langle u_i^* u_j^* \rangle}{dt} = {} & - \langle u_i^* u_l^* \rangle \frac{\partial \langle U_j \rangle}{\partial x_l} - \langle u_l^* u_j^* \rangle \frac{\partial \langle U_i \rangle}{\partial x_l} \\ & + 2 \frac{\partial \langle U_n \rangle}{\partial x_m} [\langle e_i^* u_j^* e_n^* u_m^* \rangle + \langle e_j^* u_i^* e_n^* u_m^* \rangle]. \end{aligned} \tag{40}$$

From a comparison with the physical Reynolds stress equation for RDT, Eq. (23a), the production is of the same form, while $\mathbf{M}$ is represented by a fourth-order correlation of stochastic variables (Kassinos and Reynolds[26]):

$$\begin{aligned} 2kM_{imjn} = {} & \int e_j e_n \Gamma_{im}(\mathbf{e}) dS(\mathbf{e}) \\ & \leftrightarrow \int \frac{\eta_j \eta_n}{\eta_s \eta_s} \Lambda_{im}^*(\boldsymbol{\eta}) d\boldsymbol{\eta} \\ & = \langle u_i^* u_m^* e_j^* e_n^* \rangle. \end{aligned} \tag{41}$$

Reynolds[13] and Reynolds and Kassinos[16] have defined other tensors which give additional structural information about the turbulence. The structure dimensionality tensor, $\mathbf{D}$, provides information on directions of dimensional independence, while the structure circulicity tensor, $\mathbf{F}$, provides information on the structure of the large-scale vorticity field. These variables are defined through the use of a fluctuating vector stream function, $\boldsymbol{\Psi}'$:

$$u_i = \epsilon_{ijk} \frac{\partial \Psi_k'}{\partial x_j}, \tag{42}$$

where ϵ_{ijk} is the alternating tensor. The structure tensors are defined by

$$D_{ij} \equiv \left\langle \frac{\partial \Psi_l}{\partial x_i} \frac{\partial \Psi_l}{\partial x_j} \right\rangle = \int \frac{\kappa_i \kappa_j}{\kappa^2} \Phi_{mm}(\boldsymbol{\kappa}) d\boldsymbol{\kappa}, \tag{43a}$$

and

$$F_{ij} \equiv \left\langle \frac{\partial \Psi_i}{\partial x_l} \frac{\partial \Psi_j}{\partial x_l} \right\rangle = \epsilon_{ilm} \epsilon_{jnp} \int \frac{\kappa_l \kappa_n}{\kappa^2} \Phi_{mp}(\boldsymbol{\kappa}) d\boldsymbol{\kappa}, \tag{43b}$$

where the integral relationships with the velocity spectrum apply for homogeneous turbulence. From the integral relations, the structure tensors correspond to correlations of the stochastic variables (Kassinos and Reynolds[26]):

$$D_{ij} \leftrightarrow \langle u_l^* u_l^* e_i^* e_j^* \rangle, \tag{44a}$$

and

$$F_{ij} \leftrightarrow \epsilon_{ilm} \epsilon_{jnp} \langle u_m^* u_p^* e_l^* e_n^* \rangle. \tag{44b}$$

The trace of these tensors is twice the turbulent kinetic energy as is evidenced by the stochastic model.

A geometric relation exists between the structure tensors and the Reynolds stress tensor which is shown by expressing the vector product of the alternating tensors in terms of Dirac delta functions:

$$\begin{aligned} \epsilon_{ilm} \epsilon_{jnp} = {} & \delta_{ij} (\delta_{ln} \delta_{mp} - \delta_{lp} \delta_{mn}) + \delta_{in} (\delta_{lp} \delta_{mj} - \delta_{lj} \delta_{mp}) \\ & + \delta_{ip} (\delta_{lj} \delta_{mn} - \delta_{ln} \delta_{mj}). \end{aligned} \tag{45}$$

The relation which applies for homogeneous turbulence (Kassinos and Reynolds[26]) is

$$F_{ij}+D_{ij}+\langle u_i u_j\rangle = 2k\delta_{ij}\,. \tag{46}$$

In summary, the inclusion of directional information from the evolution equation for the wave vector results in an exact PDF model for RDT, which is expressible as a model for the directional spectrum. With this model the rapid pressure–rate-of-strain correlation and the structure dimensionality and circulicity tensors are all exactly represented in the RDT limit.

IV. PDF MODEL FOR HOMOGENEOUS TURBULENCE

A. Motivation

RDT governs the behavior of turbulence in the limiting case of very strong mean distortions and is exactly represented by the **u-e** RDT Model. In the opposing limit, the energy containing scales of the turbulence have time to equilibrate with the slowly changing mean flows. This is again expressed as a condition on the normalized shear- (strain- or rotation-) rate parameter:

$$\left(\frac{Sk}{\varepsilon}\right)\ll 1. \tag{47}$$

The most basic flow of this type is decaying turbulence where there is no mean velocity gradient. Typical engineering flows are neither rapidly nor slowly distorted, but have turbulent time scales that are of the same order as the mean distortion time scale:

$$\left(\frac{Sk}{\varepsilon}\right)\sim 1. \tag{48}$$

In this section, **u-e** joint PDF models are first developed for decaying turbulence, which are combined with the **u-e** RDT Model to give general models for homogeneous turbulence.

The Reynolds stress anisotropy equation, Eq. (11), is simplified for decaying turbulence by the elimination of the production and rapid pressure–rate-of-strain correlation:

$$\frac{db_{ij}}{dt}=-\left(\frac{\varepsilon}{2k}\right)(\phi_{ij}-2b_{ij}). \tag{49}$$

The dissipation and return-to-isotropy are new terms over the RDT case and both require modeling.

The behavior of $\mathbf{e}^*$ is known for RDT, while in decaying turbulence experiments demonstrate that the return-to-isotropy tensor causes a reduction in the anisotropy of the Reynolds stresses (see Warhaft;[39] Choi and Lumley;[40] Chung and Kim[12]). A return to isotropy in the directional energy spectrum is a diffusion of the kinetic energy from some arbitrary distribution back to the isotropic, uniform distribution. This motivates the modeling of the stochastic variables, $\mathbf{e}^*$ and $\mathbf{u}^*$, by diffusional processes. When applied to the Reynolds stress equation, the diffusion of $\mathbf{e}^*$ alters the rapid pressure–rate-of-strain correlation and may be involved in modeling the return-to-isotropy tensor.

B. u-e PDF models for decaying turbulence

A general model for $\mathbf{u}^*$ and $\mathbf{e}^*$ in decaying turbulence is created from which four simplified models are also constructed. The general form for the two coupled vector-valued diffusion processes is expressed using two independent, isotropic Wiener processes, $d\mathbf{W}$ and $d\mathbf{W}'$, which gives a system of Ito stochastic differential equations (SDE's):

$$du_i^* = a_i(\mathbf{u}^*,\mathbf{e}^*)dt + A_{ij}(\mathbf{u}^*,\mathbf{e}^*)dW_j + B_{ij}(\mathbf{u}^*,\mathbf{e}^*)dW_j'\,, \tag{50a}$$

and

$$de_i^* = g_i(\mathbf{u}^*,\mathbf{e}^*)dt + G_{ij}(\mathbf{u}^*,\mathbf{e}^*)dW_j + H_{ij}(\mathbf{u}^*,\mathbf{e}^*)dW_j', \tag{50b}$$

where one of the diffusion tensors (***A***, ***B***, ***G***, or ***H***) may be arbitrarily set to zero.

Constraints on the general diffusion process are required to construct a model that is physically meaningful for decaying turbulence. Two constraints that apply for every realization of the stochastic system are required to maintain the analogy with the unit wavenumber and Fourier mode of velocity begun in the RDT model. These deterministic constraints are:

(1) $\mathbf{e}^*$ remains of unit length (by definition);
(2) $\mathbf{e}^*$ and $\mathbf{u}^*$ maintain orthogonality due to the continuity equation in Fourier space.

In addition, two statistical constraints based on physical arguments for decaying turbulence are imposed as well. They are:

(1) the PDF of velocity tends to an isotropic joint-normal distribution;
(2) the evolution of the turbulent kinetic energy is known:

$$\frac{dk}{dt}=-\varepsilon. \tag{51}$$

With these constraints the stochastic system provides realizable models for the directional spectrum and the Reynolds stresses. Also, the form of the directional spectrum model maintains continuity.

The details of the derivation are given in Appendix B, and the resulting model is summarized here:

$$du_i^* = \left(\frac{\varepsilon}{k}\right)\left[\tilde{a}_1\sqrt{k}e_i^* + \tilde{a}_2^{(1)}u_i^* + 2\tilde{a}_2^{(2)}\frac{k}{u_s^*u_s^*}u_i^* + \tilde{a}_i^a\sqrt{k}\right]dt + A_{ij}dW_j + B_{ij}dW_j'\,, \tag{52a}$$

and

$$de_i^* = \left(\frac{\varepsilon}{k}\right)\left[\tilde{g}_1 e_i^* + \tilde{g}_2\frac{u_i^*}{\sqrt{k}} + (\delta_{ij}-e_i^*e_j^*)\tilde{g}_j^a\right]dt + G_{ij}dW_j + H_{ij}dW_j'\,, \tag{52b}$$

where the coefficients are defined in Eqs. (B13), (B14), and (B16), and one constraint remains on the anisotropic drift terms:

$$\sqrt{k}\tilde{a}_l^a e_l^* + \tilde{g}_l^a u_l^* = 0. \tag{53}$$

This model is called the General **u**-**e** Decay Model, and its main purpose is to serve as a guide for the construction of simplified models that are based on assumptions into the evolution of either $\mathbf{u}^*$ or $\mathbf{e}^*$. The simplified models that are tested in this paper are given below.

1. Isotropic Diffusion of e Model (Iso)

In this model the evolution of $\mathbf{e}^*$ is taken to be an isotropic diffusion which is equivalent to a random walk of $\mathbf{e}^*$ on the unit sphere. The model has two parameters, a_u and a_e, which govern the time scales of the decay for $\mathbf{u}^*$ and $\mathbf{e}^*$, respectively. The stochastic equations are

$$du_i^* = -\tfrac{1}{2}\left(\frac{\varepsilon}{k}\right)[1+\tfrac{3}{2}a_u + a_e]u_i^* dt + \tfrac{1}{2}(a_u\varepsilon)\frac{u_i^*}{u_s^* u_s^*}\,dt - \left(\frac{a_e\varepsilon}{k}\right)^{1/2} e_i^* u_l^* dW_l + (a_u\varepsilon)^{1/2}[\delta_{il} - e_i^* e_l^*]dW_l', \tag{54a}$$

and

$$de_i^* = -\left(\frac{a_e\varepsilon}{k}\right)e_i^* dt + \left(\frac{a_e\varepsilon}{k}\right)^{1/2}[\delta_{il} - e_i^* e_l^*]dW_l. \tag{54b}$$

The return-to-isotropy tensor based on this model is a function of $\mathbf{e}^*$,

$$\phi_{ij} = (2+3a_u)b_{ij} + 2a_e(b_{ij} - d_{ij}^a) + a_u\left[\langle e_i^* e_j^*\rangle - \left\langle \frac{u_i^* u_j^*}{u_s^* u_s^*}\right\rangle\right], \tag{55}$$

where the anisotropy of the structure dimensionality tensor is defined as

$$d_{ij}^a \equiv \frac{D_{ij}}{2k} - \tfrac{1}{3}\delta_{ij}. \tag{56}$$

2. Modified Isotropic Diffusion of e Model (MIso)

In an effort to improve the Isotropic Diffusion of **e** Model, anisotropic drift terms are introduced that are proportional to the Reynolds stress anisotropy through a constant parameter, γ. The stochastic equations are

$$du_i^* = -\tfrac{1}{2}\left(\frac{\varepsilon}{k}\right)[1+\tfrac{3}{2}a_u + a_e]u_i^* dt + \left(\frac{\gamma\varepsilon}{k}\right)[b_{ij} - b_{mn}b_{mn}\delta_{ij}]u_j^* dt + \tfrac{1}{2}(a_u\varepsilon)\frac{u_i^*}{u_s^* u_s^*}dt - \left(\frac{a_e\varepsilon}{k}\right)^{1/2} e_i^* u_l^* dW_l + (a_u\varepsilon)^{1/2}[\delta_{il} - e_i^* e_l^*]dW_l', \tag{57a}$$

and

$$de_i^* = -\left(\frac{a_e\varepsilon}{k}\right)e_i^* dt - \left(\frac{\gamma\varepsilon}{k}\right)[\delta_{ij} - e_i^* e_j^*]b_{jl}e_l^* dt + \left(\frac{a_e\varepsilon}{k}\right)^{1/2}[\delta_{il} - e_i^* e_l^*]dW_l. \tag{57b}$$

The return-to-isotropy tensor based on this model is again a function of $\mathbf{e}^*$:

$$\phi_{ij} = (2+3a_u)b_{ij} + 2a_e(b_{ij} - d_{ij}^a) + a_u\left[\langle e_i^* e_j^*\rangle - \left\langle \frac{u_i^* u_j^*}{u_s^* u_s^*}\right\rangle\right] - 4\gamma[(\tfrac{1}{3} - b_{mn}b_{mn})b_{ij} + (b_{il}b_{lj} - \tfrac{1}{3}b_{mn}b_{mn}\delta_{ij})]. \tag{58}$$

3. Langevin Velocity Model (Lang)

In this model the equation for the velocity is specified as the Langevin equation with an anisotropic drift term that is proportional to the Reynolds stress anisotropy. For this model, the velocity evolution is independent of $\mathbf{e}^*$. Again, there are three parameters: a_u, a_e, and γ; which are related to the decay time scales. The stochastic equations are

$$du_i^* = -\tfrac{1}{2}\left(\frac{\varepsilon}{k}\right)[1+\tfrac{3}{2}a_u]u_i^* dt + \left(\frac{\gamma\varepsilon}{k}\right) \times [b_{ij} - b_{mn}b_{mn}\delta_{ij}]u_j^* dt + (a_u\varepsilon)^{1/2}dW_i, \tag{59a}$$

and

$$de_i^* = -\tfrac{1}{2}\left(\frac{\varepsilon}{k}\right)\left[a_e + a_u\frac{k}{u_s^* u_s^*}\right]e_i^* dt - \left(\frac{\gamma\varepsilon}{k}\right) \times [\delta_{ij} - e_i^* e_j^*]b_{jl}e_l^* dt - (a_u\varepsilon)^{1/2}\left[\frac{u_i^* e_l^*}{u_s^* u_s^*}\right]dW_l + \left(\frac{a_e\varepsilon}{k}\right)^{1/2}\left(\delta_{il} - e_i^* e_l^* - \frac{u_i^* u_l^*}{u_s^* u_s^*}\right)dW_l'. \tag{59b}$$

The return-to-isotropy model takes the standard form found in Reynolds stress closures and matches any RSM with an appropriate specification of the model parameters:

$$\phi_{ij} = (2+3a_u)b_{ij} - 4\gamma[(\tfrac{1}{3} - b_{mn}b_{mn})b_{ij} + (b_{il}b_{lj} - \tfrac{1}{3}b_{mn}b_{mn}\delta_{ij})]. \tag{60}$$

The diffusion of $\mathbf{e}^*$ affects only the rapid pressure–rate-of-strain correlation in non-decaying turbulence.

4. Structure Langevin Velocity Model (SLang)

In this model the basic Langevin equation is kept, but new anisotropic drift terms that are proportional to the anisotropic part of the structure dimensionality tensor are included. This model then has four parameters: a_u, a_e, γ_1, and γ_2; and the stochastic equations are

$$du_i^* = -\tfrac{1}{2}\left(\frac{\varepsilon}{k}\right)[1+\tfrac{3}{2}a_u]u_i^* dt + \left(\frac{\gamma_1\varepsilon}{k}\right)[b_{ij} - b_{mn}b_{mn}\delta_{ij}]u_j^* dt + \left(\frac{\gamma_2\varepsilon}{k}\right)[d_{ij}^a - b_{mn}d_{mn}^a\delta_{ij}]u_j^* dt + (a_u\varepsilon)^{1/2}dW_i, \tag{61a}$$

and

$$de_i^* = -\tfrac{1}{2}\left(\frac{\varepsilon}{k}\right)\left[a_e + a_u \frac{k}{u_s^* u_s^*}\right] e_i^* dt - \left(\frac{\gamma_1 \varepsilon}{k}\right)$$
$$\times [\delta_{ij} - e_i^* e_j^*] b_{jl} e_l^* dt - \left(\frac{\gamma_2 \varepsilon}{k}\right)[\delta_{ij}$$
$$- e_i^* e_j^*] d_{jl}^a e_l^* dt - (a_u \varepsilon)^{1/2}\left[\frac{u_i^* e_l^*}{u_s^* u_s^*}\right] dW_l$$
$$- \left(\frac{a_e \varepsilon}{k}\right)^{1/2}\left(\delta_{il} - e_i^* e_l^* - \frac{u_i^* u_l^*}{u_s^* u_s^*}\right) dW_l' . \quad (61b)$$

The return-to-isotropy tensor is then modeled as

$$\phi_{ij} = (2+3a_u) b_{ij}$$
$$- 4\gamma_1[(\tfrac{1}{3} - b_{mn}b_{mn}) b_{ij} + (b_{il}b_{lj} - \tfrac{1}{3} b_{mn}b_{mn}\delta_{ij})]$$
$$- 4\gamma_2[\tfrac{1}{3} d_{ij}^a - b_{mn} d_{mn}^a (b_{ij} + \tfrac{1}{3}\delta_{ij}) + \tfrac{1}{2}(d_{il}^a b_{lj} + d_{jl}^a b_{li})]. \quad (62)$$

C. Model performance

The models for homogeneous turbulence consist of one of the four simplified decay models combined with the RDT model. Additional closure information is also required, and it is provided by a simple dissipation model:

$$\frac{d\varepsilon}{dt} = \frac{\varepsilon^2}{k}\left(C_{\varepsilon 1}\frac{\mathbf{P}}{\varepsilon} - C_{\varepsilon 2}\right). \quad (63)$$

The parameters, $C_{\varepsilon 1}$ and $C_{\varepsilon 2}$, are set to 1.5625 and 1.9, respectively, which yield an asymptotic production-to-dissipation ratio that is representative of many flows:

$$(\mathbf{P}/\varepsilon)_\infty = \frac{C_{\varepsilon 2} - 1}{C_{\varepsilon 1} - 1} = 1.6. \quad (64)$$

This model does not take into account the decrease in dissipation that is known to occur in rotational flows, and the kinetic energy is expected to be underpredicted in these cases. Further information on modeling of the dissipation is contained in: Hanjalic and Launder[41] and Launder, Reece, and Rodi.[3]

The purpose of this work is to introduce a new methodology in turbulence modeling, and not to formulate the *ideal* model of this type. For this reason, the specification of model parameters is governed by convenience rather than the desire for optimal values. The parameters are set to yield accurate asymptotic values for the Reynolds stress anisotropy invariants for homogeneous shear flows which are important in many common engineering applications. In fact, the set of model parameters given below is not unique in its level of accuracy.

Where possible the anisotropy budgets from the models and DNS data are compared. These budgets are properly scaled and have several advantages over the unscaled Reynolds stress budgets:

(i) the anisotropy budgets for flows with different initial shear-rate parameters are directly comparable;

(ii) the asymptotic balances between terms are more apparent in the anisotropy budgets.

The anisotropy budgets also provide more rigorous tests for turbulence models than the evolution of the anisotropy, because the models for the slow and rapid terms are examined separately.

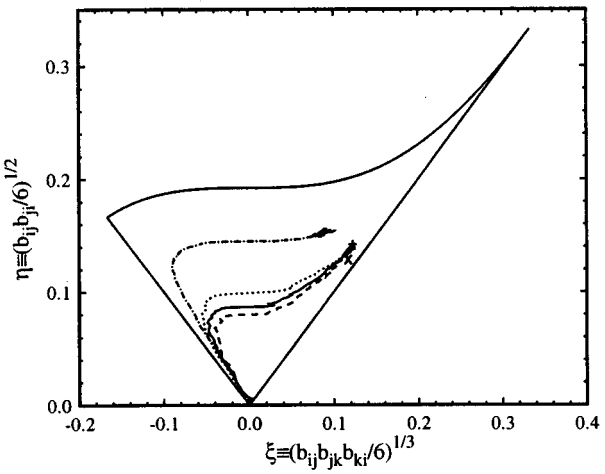

FIG. 1. Mapping of Reynolds stress anisotropy invariants in homogeneous shear with $(Sk/\varepsilon)_0 = 1.0$ for models: —, Lang; - - -, SLang; -·-, Iso; ···, MIso; compared to asymptotic states from experiments: ×, Tavoularis and Karnik (Ref. 43); and DNS: +, Rogers *et al.* (Ref. 42).

1. Homogeneous shear

Homogeneous shear flows are defined by the mean velocity gradient:

$$\frac{\partial \langle U_i \rangle}{\partial x_j} = S\begin{bmatrix} 0 & 1 & 0 \\ 0 & 0 & 0 \\ 0 & 0 & 0 \end{bmatrix}. \quad (65)$$

In Fig. 1, the trajectories of the Reynolds stress anisotropy invariants from the four models: Lang, Slang, Iso, and MIso; are presented for homogeneous shear, and the asymptotic states are compared to the DNS data from Rogers *et al.*[42] and the experimental data from Tavoularis and Karnik.[43] The model parameters are specified to yield good results for the comparison and are:

(i) Lang: $a_e = 0.03$, $a_u = 2.1$, $\gamma = 2.0$;
(ii) SLang: $a_e = 0.2$, $a_u = 2.1$, $\gamma_1 = 2.4$, $\gamma_2 = 0.2$;
(iii) Iso: $a_e = 0.3$, $a_u = 0.3$;
(iv) MIso: $a_e = 0.65$, $a_u = 1.7$, $\gamma = 2.5$.

The asymptotic states are further examined in Table I which summarizes the experimental and DNS data as well. The Lang, SLang, and MIso models are within the experimental range given, while the Iso model does not provide the proper distribution of energy between the 22 and 33 components.

Further comparisons with the DNS data of Rogers *et al.*[42] are made. In Fig. 2, the kinetic energy from the models is shown to grow much faster than that of the DNS. This defect is due to the dissipation modeling. The evolution of the Reynolds stress anisotropies for the Lang model are

TABLE I. Asymptotic values for homogeneous shear flows from: Tavoularis and Karnik (Ref. 43) (TK), Rogers, Moin, and Reynolds (Ref. 42) (RMR); Isotropic Diffusion of **e** Model (Iso); Modified Isotropic Diffusion of **e** Model (MIso); Langevin Velocity Model (Lang); Structure Langevin Velocity Model (SLang).

	TK	RMR	Iso	MIso	Lang	SLang
b_{11}^{∞}	0.18 ± 0.04	0.215	0.223	0.195	0.194	0.185
b_{12}^{∞}	-0.16 ± 0.01	-0.158	-0.156	-0.170	-0.165	-0.173
b_{22}^{∞}	-0.11 ± 0.02	-0.153	-0.203	-0.132	-0.131	-0.118
b_{33}^{∞}	-0.06 ± 0.03	-0.062	-0.020	-0.063	-0.063	-0.067
$(\mathbf{P}/\varepsilon)_{\infty}$	1.47 ± 0.14	1.80	1.6	1.6	1.6	1.6
$(Sk/\varepsilon)_{\infty}$	4.60 ± 0.14	5.7	5.12	4.72	4.83	4.62

given in Fig. 3, while their complete budgets are presented in Fig. 4. The transient results for the evolution of the anisotropies are quite good, while the asymptotic values are very good. In the anisotropy budget comparisons, the results are also quite good, especially for the asymptotic balance of terms, which are not directly forced by the selection of model parameters.

2. Homogeneous shear with frame rotation

Adding frame rotation perpendicular to the plane of the shear is a common test of turbulence models. The angular velocity is:

$$\overline{\Omega_i^f}=[0,0,\Omega^f]. \tag{66}$$

The effects of frame rotation are compared to the large-eddy simulations by Bardina, Ferziger, and Reynolds.[44] From Speziale and Mac Giolla Mhuiris,[45] the solution depends on the initial shear-rate parameter and on the rotation–to–rate-of-strain ratio, Ω^f/S. Linear stability analysis (i.e., RDT) shows that the flow is unstable with exponential growths in kinetic energy roughly in the range, $0\leqslant\Omega^f/S\leqslant0.5$.

The evolution of the kinetic energy for the Lang model is representative of all four models and is shown in Fig. 5. The model gives the correct qualitative behavior with all three cases being unstable and the energy in the $\Omega^f/S=0.25$ case growing the fastest. However, the quantitative comparison is poor which is a problem common with many second-order closures. This problem is largely attributable to the dissipation modeling.

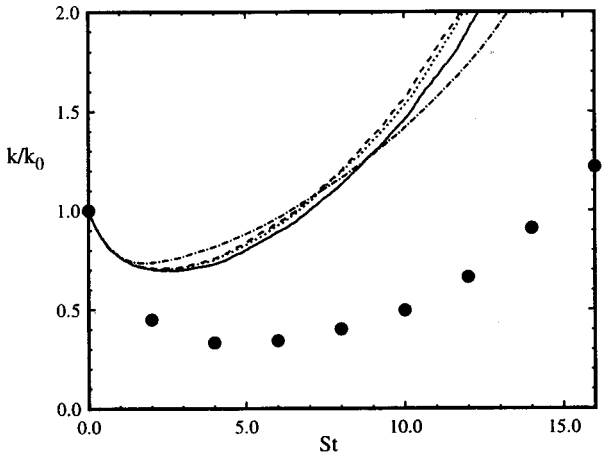

FIG. 2. Evolution of kinetic energy in homogeneous shear flow with $(Sk/\varepsilon)_0=2.36$: ●, DNS of Rogers *et al.* (Ref. 42); —, Lang; - - -, SLang; -·-, Iso; · · ·, MIso.

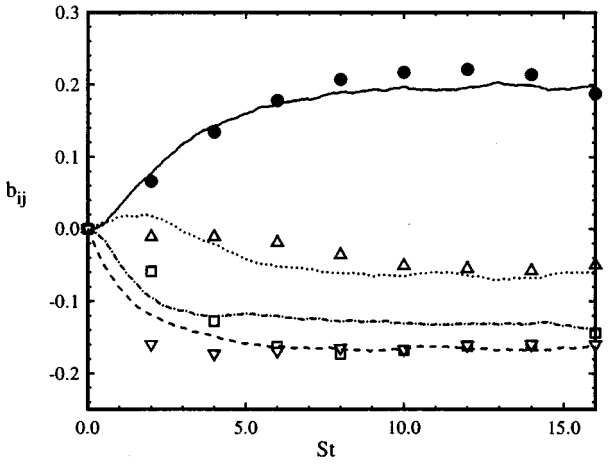

FIG. 3. Evolution of Reynolds stress anisotropy for homogeneous shear flows with $(Sk/\varepsilon)_0=2.36$. Comparison between Langevin Velocity Model (lines) and DNS of Rogers *et al.* (Ref. 42) (symbols): (—,●), b_{11}; (- - -, ∇), b_{12}; (-·-,□), b_{22}; (· · ·,△), b_{33}.

3. Axisymmetric contraction and expansion

Axisymmetric flows are specified by

$$\frac{\partial\langle U_i\rangle}{\partial x_j}=S\begin{bmatrix}1&0&0\\0&-\frac{1}{2}&0\\0&0&-\frac{1}{2}\end{bmatrix}, \tag{67}$$

with $S>0$ for contraction and $S<0$ for expansion. From symmetry the Reynolds stress anisotropy produced by these flows remains in an axisymmetric form where the only nonzero components are related by $b_{22}=b_{33}=-\frac{1}{2}b_{11}$. In addition only one component of the fourth-order tensor, **M**, is required to fully specify the rapid pressure–rate-of-strain correlation:

$$\Pi_{11}^{(r)}=12kSM_{1111}. \tag{68}$$

With these simplifications axisymmetric contraction and expansion form the two most basic irrotational flows.

The results from the models are first compared to the experimental data from Tucker[46] for axisymmetric contraction. The evolution of the kinetic energy and Reynolds stress anisotropies are presented in Figs. 6 and 7. The kinetic energy from all of the models compares with the experimental data quite well, while the anisotropies from the Lang, SLang, and MIso models yield better comparisons than the Iso model.

The case of axisymmetric contraction is also examined through the use of DNS data. The evolution of the kinetic energy from all of the models and the Reynolds stress anisotropies from the Lang and Iso models for varying initial strain-rate parameters are compared to the DNS data of Lee and Reynolds[22] in Figs. 8 and 9. The anisotropy budgets for

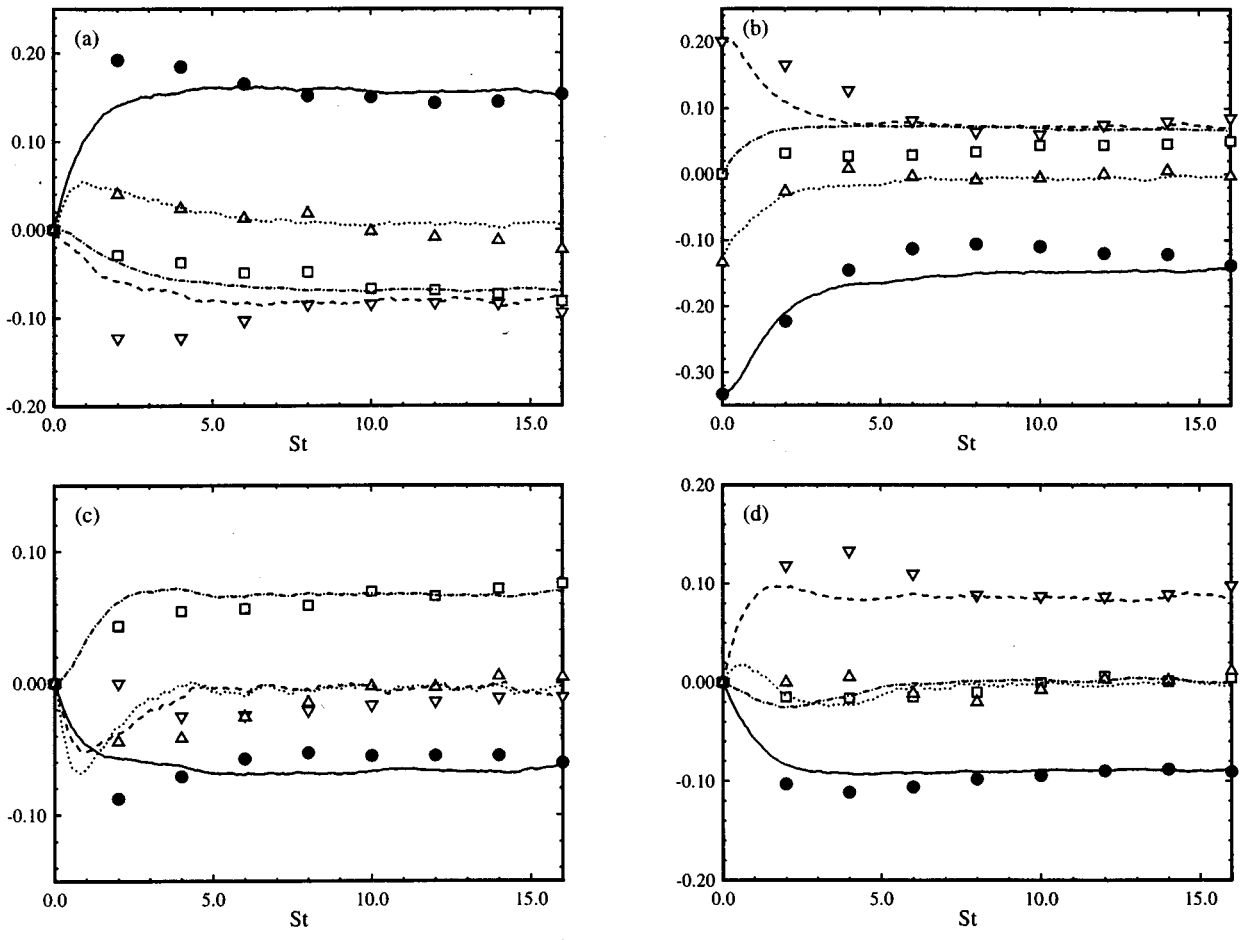

FIG. 4. Evolution of Reynolds stress anisotropy budget for homogeneous shear flows with $(Sk/\varepsilon)_0=2.36$. Comparison between Langevin Velocity Model (lines) and DNS of Rogers *et al.* (Ref. 42) (symbols): (—,●), $\mathbf{P}_{ij}^{(b)}/S$; (- - -,∇), $\mathbf{\Pi}_{ij}^{(r)}/(2kS)$; (-·-,□), $-(\varepsilon/Sk)\frac{1}{2}(\phi_{ij}-2b_{ij})$; (· · ·,△), db_{ij}/Sdt; for: (a) 11 component; (b) 12 component; (c) 22 component; (d) 33 component.

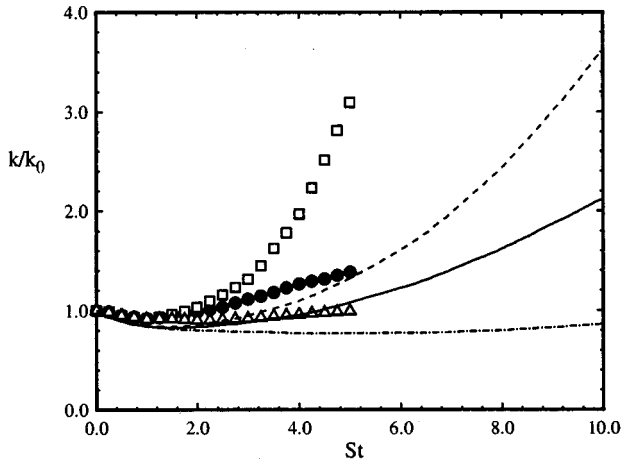

FIG. 5. Evolution of kinetic energy in homogeneous shear with a rotating frame and $(Sk/\varepsilon)_0=3.38$. Comparison between Langevin Velocity Model (lines) and LES of Bardina, Ferziger, and Reynolds (Ref. 44) (symbols): (—,●), $\Omega^f/S=0.0$; (- - -,□), $\Omega^f/S=0.25$; (-·-,△), $\Omega^f/S=0.5$.

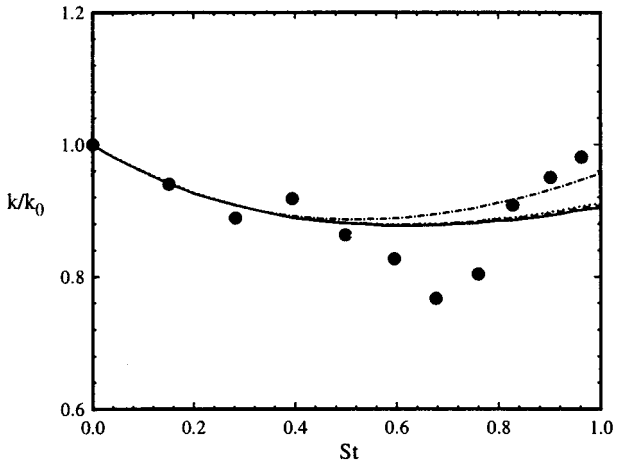

FIG. 6. Evolution of kinetic energy in axisymmetric contraction with $(Sk/\varepsilon)_0=2.1$. Comparison between the experimental data of Tucker (Ref. 46): ●, k/k_0; and the models: —, Lang; - - -, SLang; -·-, Iso; · · ·, MIso.

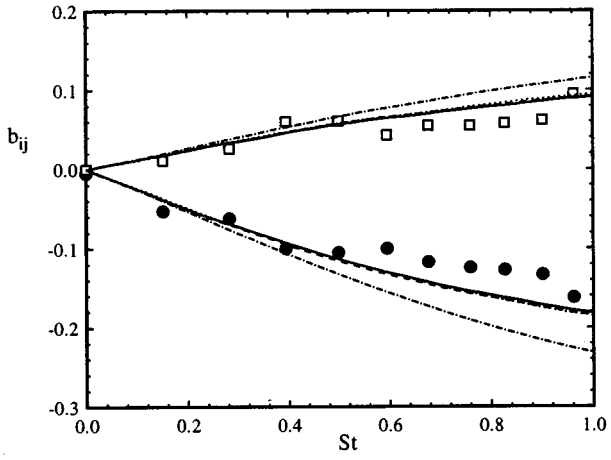

FIG. 7. Evolution of Reynolds stress anisotropy in axisymmetric contraction with $(Sk/\varepsilon)_0=2.1$. Comparison between experimental data of Tucker (Ref. 46): ●, b_{11}; □, b_{22}; and models: —, Lang; - - -, SLang; -·-, Iso; · · ·, MIso.

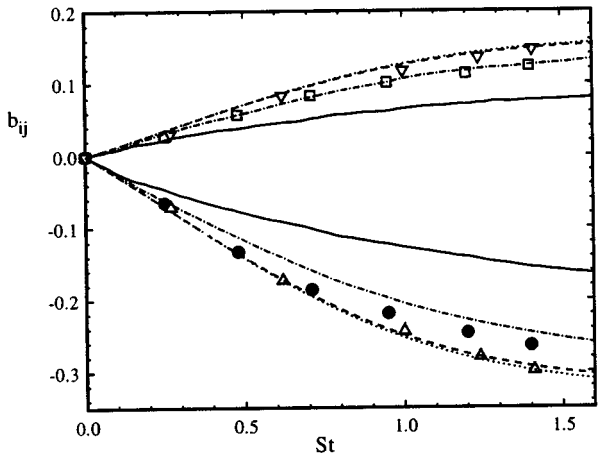

FIG. 9. Evolution of Reynolds stress anisotropies in axisymmetric contraction. Comparison between DNS of Lee and Reynolds (Ref. 22) (symbols) and models (lines) for $(Sk/\varepsilon)_0=0.557$; ●, b_{11}; □, b_{22}; —, Lang; -·-, Iso; and $(Sk/\varepsilon)_0=55.7$: △, b_{11}; ∇, b_{22}; - - -, Lang; · · ·, Iso.

the Iso model and the DNS data are also presented for two strain-rates in Fig. 10. In Fig. 11, the rapid pressure–rate-of-strain correlation is examined more closely by comparisons between the Lang and Iso models and the DNS data of Lee.[23]

The effects of the different decay models become negligible as the strain-rate increases toward the RDT limit. For this reason, all of the test results at the highest strain-rates compare with the DNS data very well. At the lower strain-rates the effects of the decay models become significant, and the models yield different results. Here, the Iso model provides the best comparisons with the DNS data, because the other models deviate from the RDT values of the rapid pressure–rate-of-strain correlation more rapidly than the DNS data indicate (see Fig. 11).

The comparisons between the models and the DNS data for axisymmetric expansion show some interesting effects. The evolution of the kinetic energy from all of the models

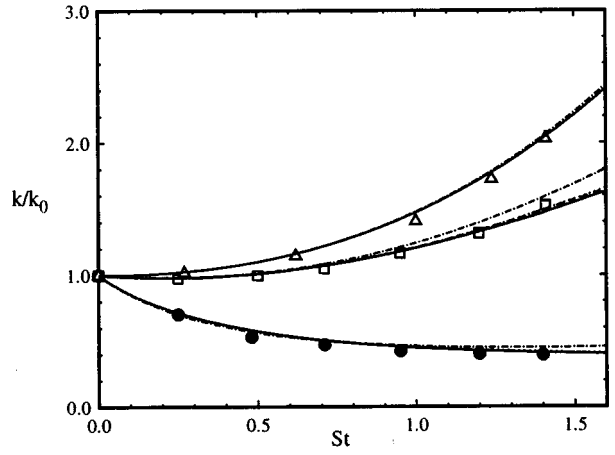

FIG. 8. Evolution of kinetic energy in axisymmetric contraction. Comparison between DNS of Lee and Reynolds (Ref. 22): ●, $(Sk/\varepsilon)_0=0.557$; □, $(Sk/\varepsilon)_0=5.57$; △, $(Sk/\varepsilon)_0=55.7$; and models: —, Lang; - - -, SLang; -·-, Iso; · · ·, MIso.

and the Reynolds stress anisotropies from the Lang and Iso models for varying initial strain-rate parameters are compared to the DNS data of Lee and Reynolds[22] in Figs. 12 and 13. In the energy comparison the models do very well for $St<1.0$, but deviate even for the highest strain-rate for $St>1.0$. This degradation of the solution is due to an instability that exists for axisymmetric expansion in RDT which was described by Kassinos and Reynolds.[27]

The models give anisotropies that decrease as the initial strain-rate parameter decreases, while DNS shows the non-intuitive tendency to have increased anisotropies for decreased strain-rates. To understand the evolution of the anisotropies, their budgets for the Iso model and the DNS data are compared in Fig. 14. The modeled rapid pressure–rate-of-strain correlation and the closed production terms compare very well. This point is further emphasized in Fig. 15 by comparing the rapid pressure–rate-of-strain correlation from the Lang and Iso models to the DNS data of Lee.[23] Although the Iso model performs better, the Lang model is still reasonable. It is actually the slow terms that cause the difference in the anisotropy evolutions. For the DNS data these terms *increase* the anisotropy; i.e., drive the system from isotropy.

The slow terms include the return-to-isotropy tensor and the Reynolds stress anisotropy which is a scaling term due to the dissipation of the kinetic energy. In Fig. 16, the differences between the Iso model and the DNS data are apparent. Since the anisotropy is a closed term, the source of the trouble is the modeling for the return-to-isotropy tensor.

These results have significant implications for the modeling of the return-to-isotropy tensor. In Reynolds stress closures, this tensor is modeled as a function of the anisotropy. Some of the latest models (Chung and Kim[12]) include model coefficients that depend on the Reynolds number and anisotropy invariants. However, the resulting parameters are specified with comparisons to decaying turbulence and maintain slow terms that strictly reduce the anisotropy for all Reynolds numbers. The DNS results of Lee and Reynolds[22] in-

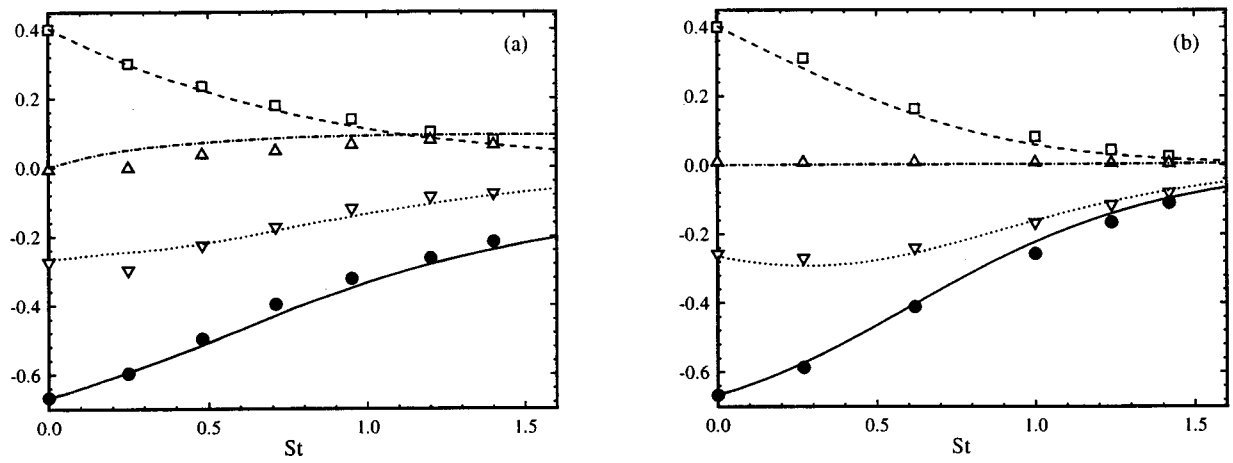

FIG. 10. Evolution of Reynolds stress anisotropy budget in axisymmetric contraction. Comparison between Isotropic Diffusion of **e** Model (lines) and DNS of Lee and Reynolds (Ref. 22) (symbols): (—,●), $\mathbf{P}_{11}^{(b)}/S$; (- - -,□), $\mathbf{\Pi}_{11}^{(r)}/(2kS)$; (-·-,△), $-(\varepsilon/Sk)\frac{1}{2}(\phi_{11}-2b_{11})$; (···,∇), db_{11}/Sdt; for: (a) $(Sk/\varepsilon)_0=0.557$; (b) $(Sk/\varepsilon)_0=55.7$.

dicate that this is not always the case for homogeneous turbulence.

4. Elliptical flows

Flows with elliptical streamlines are generated by the mean velocity gradient:

$$\frac{\partial\langle U_i\rangle}{\partial x_j}=\begin{bmatrix}0 & S+\omega & 0\\ S-\omega & 0 & 0\\ 0 & 0 & 0\end{bmatrix}, \tag{69}$$

with $|\omega|>|S|$, while $|\omega|<|S|$ generates hyperbolic streamlines. The flow is a combination of plane strain and solid body rotation and is also parameterized through the aspect ratio of the elliptical streamlines, $E\equiv\sqrt{(S+\omega)/(\omega-S)}$, and the rotation frequency, $\Omega\equiv\sqrt{(S+\omega)(\omega-S)}$ (Blaisdell and Shariff[47]). Stability issues for the elliptical flows were addressed in the following references: Cambon, Teissèdre, and Jeandel;[48] Pierrehumbert;[49] Bayly;[50] Landman and Saffman;[51] and Waleffe;[52] and the results show that the flow is unstable with exponential growths in kinetic energy for all values of $(\omega/S)=(E^2+1)/(E^2-1)>1$. However, Speziale, Abid, and Blaisdell[17] have shown that current second-order closures predict that the flows restabilize for $\omega/S\leqslant 2$ for any initial mean rotation-rate parameter, $(\Omega k/\varepsilon)_0$.

The models were tested in a case with nearly circular streamlines, $E=1.1$, and a high initial rotation-rate parameter, $(\Omega k/\varepsilon)_0=270$. In this case, the rotation–to–rate-of-strain ratio is large, $(\omega/S)=10.5$, for which all second-order closures erroneously predict decaying kinetic energy. Figure 17 does show growing kinetic energy in all four models, but the rates are far lower than the exponential growth found in the DNS data of Blaisdell and Shariff[47] for $(\Omega k/\varepsilon)_0=4.05$ (not shown). The poor quantitative results are at least partially due to the dissipation model which ignores the known decrease in dissipation due to rotation.

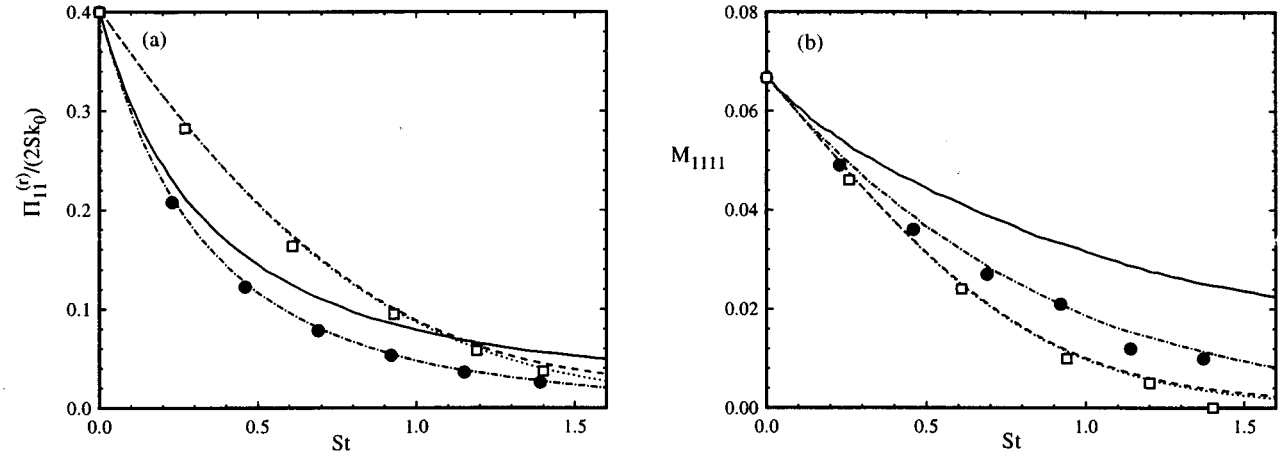

FIG. 11. Evolution of (a) normalized rapid pressure–rate-of-strain correlation; (b) Fourth-order correlation; in axisymmetric contraction. Comparison between DNS of Lee (Ref. 23) and models with $(Sk/\varepsilon)_0=0.5$: ●, DNS; —, Lang; -·-, Iso; and $(Sk/\varepsilon)_0=50.0$ □, DNS; - - -, Lang ···, Iso.

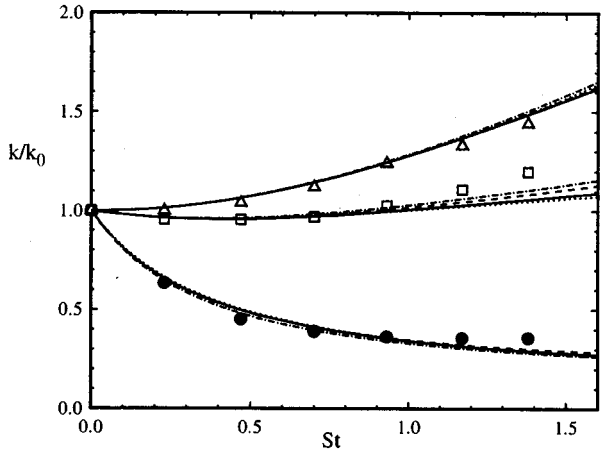

FIG. 12. Evolution of kinetic energy in axisymmetric expansion. Comparison between DNS of Lee and Reynolds (Ref. 22): ●, $(Sk/\varepsilon)_0=0.408$; □, $(Sk/\varepsilon)_0=4.08$; △, $(Sk/\varepsilon)_0=40.8$; and models: —, Lang; - - -, SLang; -·-, Iso; · · ·, MIso.

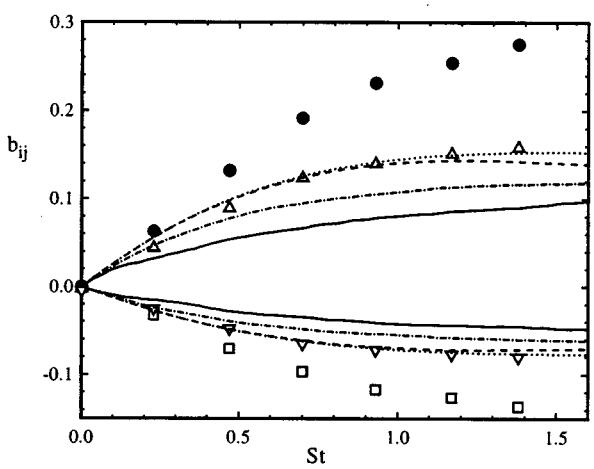

FIG. 13. Evolution of Reynolds stress anisotropies in axisymmetric expansion. Comparison between DNS of Lee and Reynolds (Ref. 22) (symbols) and models (lines) for $(Sk/\varepsilon)_0=0.408$: ●, b_{11}; □, b_{22}; —, Lang; -·-, Iso; and $(Sk/\varepsilon)_0=40.8$: △, b_{11}; ∇, b_{22}; - - -, Lang; · · ·, Iso.

5. Model comparison

In summary, the four models with their specified sets of parameters provide very good results in all test flows at the highest strain-rates where the flows are nearly in the RDT limit. At lower strain-rates, all the models provide quite good results in all of the test flows except axisymmetric expansion. It has been shown in this case that the problems are caused by poor modeling of the return-to-isotropy tensor and that RSM's which are based on decaying turbulence share these problems. Because the models directly impact the anisotropy budgets, the differences between the models are more apparent in the anisotropies than in the kinetic energies.

The Lang, Slang, and MIso models yield similar results due to the comparable parameter values for the anisotropic drift terms that are proportional to the Reynolds stress anisotropy. These models perform better in homogeneous shear and axisymmetric contraction when compared to experimental data, while the Iso model performs better in axisymmetric expansion and contraction when compared to DNS data. The Iso model is better in these cases, because it matches the DNS data in deviating from RDT more slowly than the other three models. It is possible that the very low Reynolds numbers of the DNS is a factor in this result. Because of its inferior performance for the important case of homogeneous shear, the Iso model is not recommended for future use.

The modeled return-to-isotropy tensors are one way to differentiate between the four models. The modeled tensors from the Iso and MIso models contain expectations which do not have good physical interpretations, while the tensor from the Lang model takes the general form for RSM's if the parameters are allowed to be functions of the anisotropy invariants and Reynolds number. The SLang model includes effects of the structure dimensionality anisotropy tensor, but

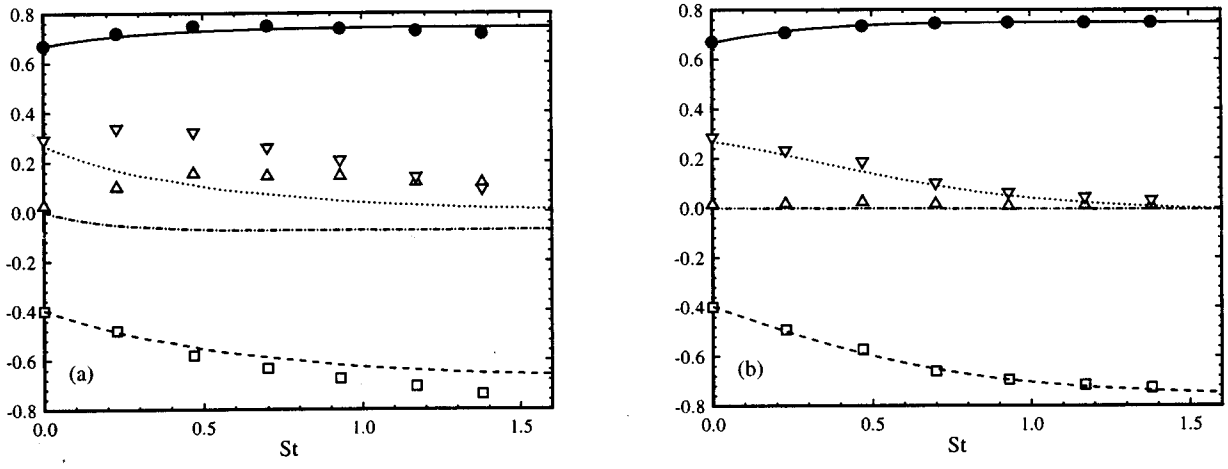

FIG. 14. Evolution of Reynolds stress anisotropy budget in axisymmetric expansion. Comparison between Isotropic Diffusion of **e** Model (lines) and DNS of Lee and Reynolds (Ref. 22) (symbols): (—,●), $\mathbf{P}_{11}^{(b)}/|S|$; (- - -,□), $\mathbf{\Pi}_{11}^{(r)}/(2k|S|)$; (-·-,△), $-(\varepsilon/|S|k)\frac{1}{2}(\phi_{11}-2b_{11})$; (· · ·,∇), $db_{11}/|S|dt$; for: (a) $(Sk/\varepsilon)_0=0.408$; (b) $(Sk/\varepsilon)_0=40.8$.

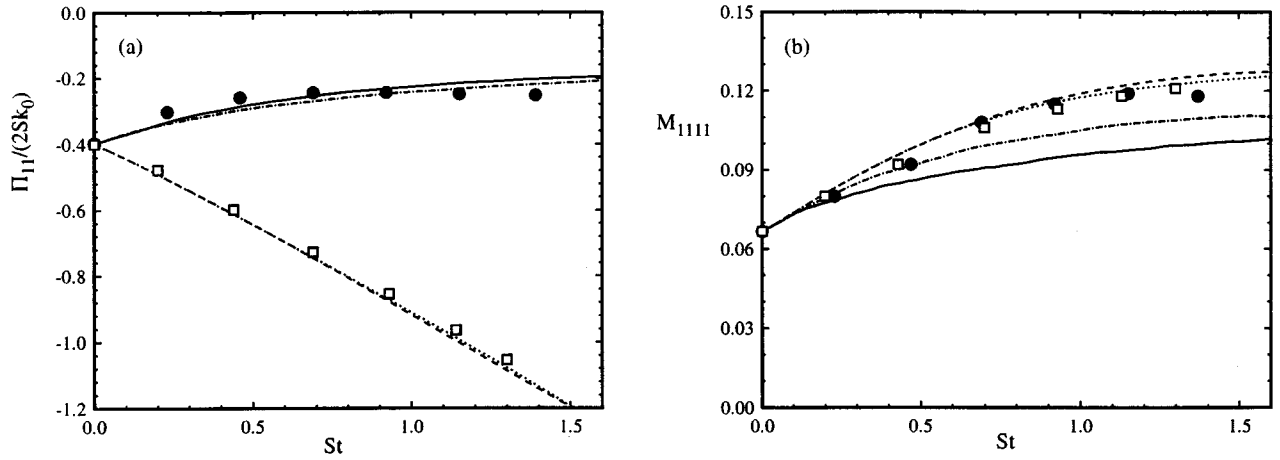

FIG. 15. Evolution of (a) normalized rapid pressure–rate-of-strain correlation; (b) Fourth-order correlation; in axisymmetric expansion. Comparison between DNS of Lee (Ref. 23) and models with $(Sk/\varepsilon)_0=0.5$: ●, DNS; —, Lang; -·-, Iso; and $(Sk/\varepsilon)_0=50.0$ □, DNS; - - -, Lang ···, Iso.

does not provide a general model of the form: $\phi_{ij}=\phi_{ij}(\mathbf{b}, \mathbf{d}^a)$. A general model of this form could be created and might provide improved modeling for the return-to-isotropy tensor. However, the SLang model in its current form does not significantly improve over the Lang model. For our future work in inhomogeneous turbulence, the Lang model will be used, because the evidence so far does not indicate an advantage in using the more complicated SLang or MIso models.

V. PDF MODEL FOR INHOMOGENEOUS TURBULENCE

In this section the **u**-**e** PDF model for rapidly distorted inhomogeneous turbulence is constructed based on the RDT model for the homogeneous case from Sec. III C. The general PDF models for non-rapid inhomogeneous turbulence are not presented but follow directly by adding a decay model from Sec. IV B.

In PDF methods of inhomogeneous turbulence it is useful to view the stochastic equations as models for Lagrangian fluid particles. In a Lagrangian system, the particle position, $\mathbf{X}^+(t,\mathbf{Y})$, evolves by the particle velocity, $\mathbf{U}^+(t,\mathbf{Y}) \equiv \mathbf{U}(\mathbf{X}^+[t,\mathbf{Y}],t)$:

$$\frac{\partial X_i^+}{\partial t}=U_i^+, \tag{70}$$

where $\mathbf{Y}$ is the particle position at a reference time. Also, the local Lagrangian excess velocity is defined by

$$\begin{aligned}\mathbf{u}^+(t,\mathbf{Y}) &\equiv \mathbf{U}^+(t,\mathbf{Y})-\langle \mathbf{U}(\mathbf{x},t)\rangle_{\mathbf{x}=\mathbf{X}^+(t,\mathbf{Y})}\\ &=\mathbf{u}(\mathbf{X}^+[t,\mathbf{Y}],t),\end{aligned} \tag{71}$$

where $\mathbf{u}(\mathbf{x},t)$ is the Eulerian fluctuating velocity.

From the Navier-Stokes equations expressed as

$$\frac{DU_i}{Dt}=-\frac{\partial\langle P\rangle}{\partial x_i}-\frac{\partial P'}{\partial x_i}+\nu\frac{\partial^2 U_i}{\partial x_l \partial x_l}\equiv-\frac{\partial\langle P\rangle}{\partial x_i}+a_i, \tag{72}$$

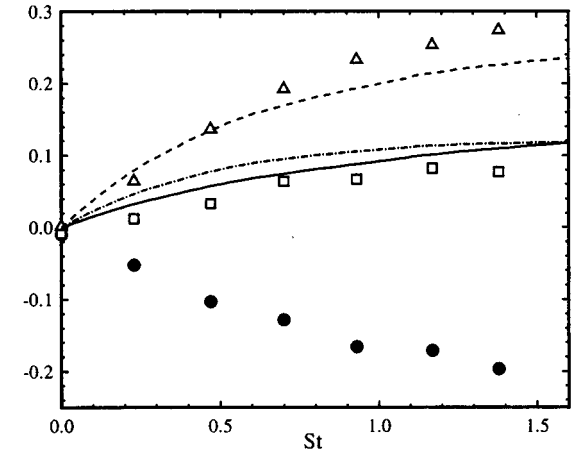

FIG. 16. Evolution of the slow terms in axisymmetric expansion. Comparison between DNS of Lee and Reynolds (Ref. 22) (symbols) and Iso model (lines) with $(Sk/\varepsilon)_0=0.408$: (—,●), $\frac{1}{2}(\phi_{11}-2b_{11})$; (- - -,□), $\phi_{11}/2$; (-·-, △), b_{11}.

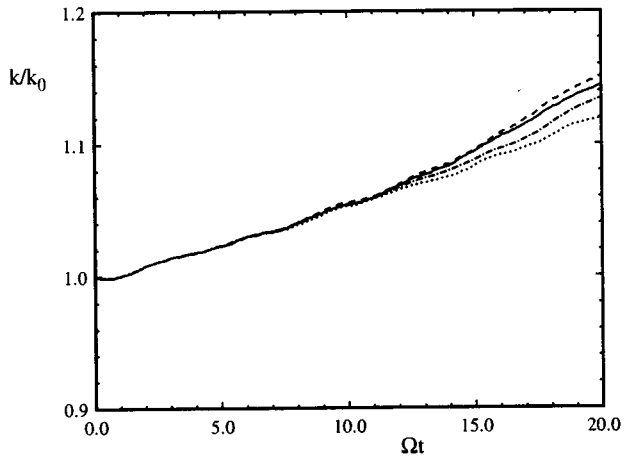

FIG. 17. Evolution of kinetic energy in an elliptical flow with $\omega/S=10.5$: —, Lang model; - - -, Slang model; -·-, Iso model; ···, MIso model.

the equation for the Lagrangian velocity is

$$\frac{\partial U_i^+}{\partial t} = \left\{ \frac{DU_i}{Dt} \right\}_{\mathbf{x}=\mathbf{X}^+(t,\mathbf{Y})} = \left\{ -\frac{\partial \langle P \rangle}{\partial x_i} \right\}_{\mathbf{x}=\mathbf{X}^+(t,\mathbf{Y})} + a_i(\mathbf{X}^+[t,\mathbf{Y}],t). \tag{73}$$

The effects of viscosity on the mean velocity is negligible at high Reynolds numbers which results in $\langle \mathbf{a} \rangle = 0$. The equation for the Lagrangian excess velocity is then

$$\frac{\partial u_i^+}{\partial t} = \left\{ \frac{Du_i}{Dt} \right\}_{\mathbf{x}=\mathbf{X}^+(t,\mathbf{Y})} = \left\{ \frac{\partial \langle u_i u_l \rangle}{\partial x_l} - u_l \frac{\partial \langle U_i \rangle}{\partial x_l} \right\}_{\mathbf{x}=\mathbf{X}^+(t,\mathbf{Y})} + a_i(\mathbf{X}^+[t,\mathbf{Y}],t), \tag{74}$$

where the first two terms account for the changing velocity due to the particle's movement.

The stochastic representation of $(\mathbf{X}^+, \mathbf{U}^+, \mathbf{u}^+)$ is $(\mathbf{X}^*, \mathbf{U}^*, \mathbf{u}^*)$ for which a model of $\mathbf{a}$ is required. The evolution of the stochastic position is simply

$$dX_i^* = U_i^* dt. \tag{75}$$

The equations for $\mathbf{U}^*$ are constructed in a manner that yields the RDT model for $\mathbf{u}^*$ in homogeneous turbulence, Eq. (34a). The velocity model is

$$dU_i^* = -\frac{\partial \langle P \rangle}{\partial x_i} dt + 2 \frac{\partial \langle U_m \rangle}{\partial x_n} [e_i^* e_m^* u_n^* - \langle e_i^* e_m^* u_n^* \rangle] dt, \tag{76}$$

where the corresponding model of $\mathbf{u}^*$ is

$$du_i^* = -\frac{\partial \langle U_m \rangle}{\partial x_n} u_n^* (\delta_{im} - 2 e_i^* e_m^*) dt - 2 \frac{\partial \langle U_m \rangle}{\partial x_n} \langle e_i^* e_m^* u_n^* \rangle dt + \frac{\partial \langle u_i u_j \rangle}{\partial x_j} dt. \tag{77}$$

This equation reduces to the velocity RDT equation, Eq. (34a), in homogeneous turbulence because the gradients of the Reynolds stress are zero and the triple correlation, $\langle e_i^* e_m^* u_n^* \rangle$, is also zero by symmetry in the velocity distribution. The triple correlation term was added to Eq. (76) to force the exact evolution equation for the mean Eulerian velocity, which is equivalent to forcing the mean of the modeled $\mathbf{a}$ to be zero.

The evolution equation for the wave vector follows by maintaining a unit length and orthogonality with $\mathbf{u}^*$:

$$de_i^* = -\frac{\partial \langle U_m \rangle}{\partial x_n} e_m^* (\delta_{in} - e_i^* e_n^*) dt - \left[\frac{\partial \langle u_l u_j \rangle}{\partial x_j} - 2 \frac{\partial \langle U_m \rangle}{\partial x_n} \langle e_l^* e_m^* u_n^* \rangle \right] \frac{e_l^* u_i^*}{u_s^* u_s^*} dt. \tag{78}$$

The final term in this equation corresponds to the inhomogeneous terms in Eq. (77) and has the purpose of maintaining the wave vector in the plane orthogonal to the excess velocity. A direct calculation of this projection during the Monte Carlo simulation is equally valid and preferable numerically due to the high statistical error inherent in calculating the gradients of the Reynolds stresses.

VI. CONCLUSIONS

A new approach to PDF modeling of inhomogeneous turbulence has been developed that provides exact representation of rapidly distorted homogeneous turbulence. The construction is based on the particle representation model by Kassinos and Reynolds.[26] Their approach is adapted into a PDF formulation that begins with a model for the joint PDF of a velocity Fourier mode and unit wavenumber vector. This is an exact representation of RDT at the level of the directional spectrum. To provide an initial condition for the Monte Carlo solution of this PDF method, an algorithm is also presented that generates a stochastic system in Fourier space that corresponds to a homogeneous vector field with a prescribed spectrum.

An equivalent formulation of the RDT model using physical space variables is required for the extension of the method to the inhomogeneous case. The result is a model for the joint PDF of the velocity and wave vector, the **u-e** RDT Model, which is based on the integral relationship between the directional spectrum and the Reynolds stresses (Kassinos and Reynolds[26]). A difference between PDF methods based on the **u-e** RDT Model and standard PDF methods is that the model for the rapid pressure term in the PDF of velocity equation corresponds to a model for the directional spectrum and not just the Reynolds stresses. Because the directional spectrum is a complete description for RDT, this limit is now treated exactly.

Models for general homogeneous turbulence are constructed by combining the **u-e** RDT Model with a **u-e** model for decaying turbulence. The decay models maintain the analogy with the directional spectrum through two deterministic constraints: **e** is of unit length and **u-e** are orthogonal; and the analogy with the particle velocities through two statistical constraints: the joint PDF of **u** tends to a joint normal distribution in isotropic turbulence and the kinetic energy evolves by the dissipation. By maintaining these analogies the PDF method can be viewed either as stochastic model for fluid particles in physical space or as a realizable spectral model at the level of the directional spectrum.

Five models for decaying turbulence are constructed: General **u-e** Decay Model, Isotropic Diffusion of **e** Model (Iso), Modified Isotropic Diffusion of **e** Model (MIso), Langevin Velocity Model (Lang), and Structure-Langevin Velocity Model (SLang). The Lang, SLang, Iso, and MIso models perform quite well in the cases of homogeneous turbulence that are tested. The Lang, SLang, and MIso models provide very similar results in all cases and are better than the Iso model in the important case of homogeneous shear. The Lang model is currently preferable, because it yields the general form for the return-to-isotropy tensor used in RSM's. A future version of the SLang model may provide better modeling of this tensor.

The extension of the homogeneous turbulence models to models for inhomogeneous turbulence is accomplished by adding a stochastic variable representing the particle location and through the use of the full particle velocity. The resulting models maintain the exact solution for RDT of homogeneous turbulence.

While testing the homogeneous models, several general

observations were made about turbulence modeling. It was argued that the anisotropy budgets are important means of comparing turbulence models to DNS data, because they are properly scaled and allow separate comparisons for the slow and rapid models. Therefore, they form a more rigorous test than the anisotropy evolutions. From the anisotropy budgets of axisymmetric expansion, it is shown that the increase in anisotropy for lower initial strain-rates is caused by the slow terms. In particular, the scaling term from the dissipation of kinetic energy is larger than the return-to-isotropy tensor. This presents a problem for all models of the return-to-isotropy tensor that are based on decaying turbulence where this effect has not been observed. Also, the need for an improved dissipation model is apparent, especially in the cases where rotational effects are important.

ACKNOWLEDGMENTS

This work was supported in part by the Department of Defense through the Air Force Graduate Fellowship Program and in part by the Air Force Office of Scientific Research, Grant F49620-94-1-0098.

APPENDIX A: SYNTHESIS OF HOMOGENEOUS RANDOM VECTOR FIELDS WITH A PRESCRIBED SPECTRUM

The purpose of this appendix is to show how to synthesize a random field as the sum of N conjugate pairs of independent modes such that its two-point correlation converges to a specified one as N tends to infinity.

Let $\boldsymbol{u}(\boldsymbol{x})$ be a real, zero-mean, statistically-homogeneous random vector field with spectrum function, $\Phi_{ij}(\boldsymbol{\kappa})$. The two-point correlation and the spectrum are related by Eq. (12) or its inverse

$$R_{ij}(\boldsymbol{r}) \equiv \langle u_i(\boldsymbol{x}) u_j(\boldsymbol{x}+\boldsymbol{r}) \rangle = \int \Phi_{ij}(\boldsymbol{\kappa}) e^{\imath \boldsymbol{\kappa}\cdot\boldsymbol{r}} d\boldsymbol{\kappa}. \tag{A1}$$

From conjugate symmetry and an additional symmetry condition from homogeneity, the real and symmetric parts of the spectrum are equivalent:

$$\mathrm{Re}\{\Phi_{ij}(\boldsymbol{\kappa})\} = \Phi^s_{ij}(\boldsymbol{\kappa}) \equiv \tfrac{1}{2}[\Phi_{ij}(\boldsymbol{\kappa}) + \Phi_{ji}(\boldsymbol{\kappa})], \tag{A2a}$$

while the imaginary and anti-symmetric part are related by

$$\imath\ \mathrm{Im}\{\Phi_{ij}(\boldsymbol{\kappa})\} = \Phi^a_{ij}(\boldsymbol{\kappa}) \equiv \tfrac{1}{2}[\Phi_{ij}(\boldsymbol{\kappa}) - \Phi_{ji}(\boldsymbol{\kappa})]. \tag{A2b}$$

The terms in Eq. (A2a) are called the co-spectrum, while the terms in Eq. (A2b) are called the quadrature spectrum. These relations show that the spectrum tensor forms a Hermitian matrix. Further, because the spectrum is a representation of the energy at a particular location in Fourier space, the matrix is also positive semi-definite (Batchelor[36]).

The energy of the random vector field is defined via

$$k \equiv \int \tfrac{1}{2}\Phi_{ll}(\boldsymbol{\kappa}) d\boldsymbol{\kappa}, \tag{A3}$$

with which a normalized spectrum is defined by

$$f(\boldsymbol{\kappa}) \equiv \tfrac{1}{2}\Phi_{ll}(\boldsymbol{\kappa})/k. \tag{A4}$$

The normalized spectrum is non-negative and integrates to unity; i.e., it has the properties of a joint PDF. Another normalized spectrum is also defined by

$$\Psi_{ij}(\boldsymbol{\kappa}) \equiv \Phi_{ij}(\boldsymbol{\kappa})/\Phi_{ll}(\boldsymbol{\kappa}). \tag{A5}$$

In terms of these the normalized spectra, Eq. (A1) is rewritten:

$$R_{ij}(\boldsymbol{r}) = 2k \int \Psi_{ij}(\boldsymbol{\kappa}) e^{\imath \boldsymbol{\kappa}\cdot\boldsymbol{r}} f(\boldsymbol{\kappa}) d\boldsymbol{\kappa}. \tag{A6}$$

If $\boldsymbol{\kappa}^*$ is defined to be a random vector with a joint PDF of $f(\boldsymbol{\kappa})$, then the integral in Eq. (A6) is equivalent to an expectation:

$$R_{ij}(\boldsymbol{r}) = 2k \langle \Psi_{ij}(\boldsymbol{\kappa}^*) e^{\imath \boldsymbol{\kappa}^*\cdot\boldsymbol{r}} \rangle. \tag{A7}$$

The synthetic field, $\tilde{\boldsymbol{u}}(\boldsymbol{x})$, is defined for a given N by

$$\tilde{\boldsymbol{u}}(\boldsymbol{x}) \equiv \frac{1}{\sqrt{2N}} \sum_{n=-N}^{N} \boldsymbol{Z}^{(n)} e^{\imath \boldsymbol{\kappa}^{(n)}\cdot\boldsymbol{x}}, \tag{A8}$$

where $\boldsymbol{\kappa}^{(n)}$ are independent and identically distributed wavenumber vectors with distribution $f(\boldsymbol{\kappa})$ and $\boldsymbol{Z}^{(n)}$ are identically distributed zero-mean random vectors, dependent on $\boldsymbol{\kappa}^{(n)}$, whose covariance matrix is deduced below, Eq. (A12). In addition, conjugate symmetry is guaranteed by using conjugate pairs:

$$\boldsymbol{Z}^{(-n)} \equiv (\boldsymbol{Z}^{(n)})^* \quad \text{and} \quad \boldsymbol{\kappa}^{(-n)} \equiv -\boldsymbol{\kappa}^{(n)}, \quad \text{for } n = 1,N. \tag{A9}$$

The complex conjugate of Eq. (A8) provides an alternate definition of the field:

$$\tilde{\boldsymbol{u}}(\boldsymbol{x}) \equiv \frac{1}{\sqrt{2N}} \sum_{n=-N}^{N} (\boldsymbol{Z}^{(n)})^* e^{-\imath \boldsymbol{\kappa}^{(n)}\cdot\boldsymbol{x}}. \tag{A10}$$

From Eqs. (A8) and (A10), the two-point correlation of the synthetic field is

$$\begin{aligned} \tilde{R}_{ij}(\boldsymbol{r}) &\equiv \langle \tilde{u}_i(\boldsymbol{x}) \tilde{u}_j(\boldsymbol{x}+\boldsymbol{r}) \rangle \\ &= \frac{1}{2N} \sum_{n=-N}^{N} \langle (Z_i^{(n)})^* Z_j^{(n)} e^{\imath \boldsymbol{\kappa}^{(n)}\cdot\boldsymbol{r}} \rangle. \end{aligned} \tag{A11}$$

By comparing Eqs. (A7) and (A11), we observe that $\tilde{R}_{ij}(\boldsymbol{r},t)$ equals $R_{ij}(\boldsymbol{r},t)$ (for all $N \geqslant 1$) provided $\boldsymbol{Z}^{(n)}$ satisfies

$$\langle (Z_i^{(n)})^* Z_j^{(n)} | \boldsymbol{\kappa}^{(n)} = \boldsymbol{\kappa} \rangle = 2k \Psi_{ij}(\boldsymbol{\kappa}). \tag{A12}$$

The complex random vectors, $\boldsymbol{Z}^{(n)}$, must have a covariance matrix given by Eq. (A12), but their distribution is not determined. It is convenient to specify $\boldsymbol{Z}^{(n)}$ as Gaussian random vectors, because the distribution is then determined from the covariance matrix. In practice, $\boldsymbol{Z}^{(n)}$ can be constructed from real, standard, isotropic Gaussian random vectors, $\boldsymbol{\xi}^{(n)}$, by

$$\boldsymbol{Z}^{(n)} = (\boldsymbol{L})^* \boldsymbol{\xi}^{(n)}, \tag{A13}$$

where $\boldsymbol{L}$ is a complex triangular matrix with a real diagonal that is uniquely defined by

$$\langle (\boldsymbol{Z}^{(n)})^* \boldsymbol{Z}^{(n)T} | \boldsymbol{\kappa}^{(n)} = \boldsymbol{\kappa} \rangle = \boldsymbol{L}(\boldsymbol{L})^{*T} = 2k \Psi_{ij}(\boldsymbol{\kappa}). \tag{A14}$$

This is simply the complex version of the Cholesky factorization for positive, semi-definite, Hermitian matrices.

APPENDIX B: CONSTRUCTION OF GENERAL u-e DECAY MODEL

A general model for $\mathbf{u}^*$ and $\mathbf{e}^*$ in decaying turbulence is constructed based on the form for coupled stochastic diffusion processes:

$$du_i^* = a_i(\mathbf{u}^*,\mathbf{e}^*)dt + A_{ij}(\mathbf{u}^*,\mathbf{e}^*)dW_j + B_{ij}(\mathbf{u}^*,\mathbf{e}^*)dW_j', \tag{B1a}$$

and

$$de_i^* = g_i(\mathbf{u}^*,\mathbf{e}^*)dt + G_{ij}(\mathbf{u}^*,\mathbf{e}^*)dW_j + H_{ij}(\mathbf{u}^*,\mathbf{e}^*)dW_j', \tag{B1b}$$

and the four constraints given in Sec. IV B. In applying these constraints to the diffusion process some simplifying assumptions are made in order to achieve a tractable model. As a result the General **u-e** Decay Model is not in the *most* general form, but maintains more than sufficient generality for our purposes.

Before the constraints are applied to the diffusion process, its coefficients are re-expressed using the isotropic functions of $\mathbf{u}^*$ and $\mathbf{e}^*$:

$$a_i(\mathbf{u}^*,\mathbf{e}^*) = a_1 e_i^* + a_2 u_i^* + a_i^a, \tag{B2a}$$

$$g_i(\mathbf{u}^*,\mathbf{e}^*) = g_1 e_i^* + g_2 u_i^* + g_i^a, \tag{B2b}$$

$$A_{ij}(\mathbf{u}^*,\mathbf{e}^*) = \mathscr{A}_1\delta_{ij} + \mathscr{A}_2 e_i^* e_j^* + \mathscr{A}_3\frac{u_i^* u_j^*}{u_s^* u_s^*} + \mathscr{A}_4 e_i^* u_j^* + \mathscr{A}_5 e_j^* u_i^* + A_{ij}^a, \tag{B2c}$$

$$B_{ij}(\mathbf{u}^*,\mathbf{e}^*) = \mathscr{B}_1\delta_{ij} + \mathscr{B}_2 e_i^* e_j^* + \mathscr{B}_3\frac{u_i^* u_j^*}{u_s^* u_s^*} + \mathscr{B}_4 e_i^* u_j^* + \mathscr{B}_5 e_j^* u_i^* + B_{ij}^a, \tag{B2d}$$

$$G_{ij}(\mathbf{u}^*,\mathbf{e}^*) = \mathscr{G}_1\delta_{ij} + \mathscr{G}_2 e_i^* e_j^* + \mathscr{G}_3\frac{u_i^* u_j^*}{u_s^* u_s^*} + \mathscr{G}_4 e_i^* u_j^* + \mathscr{G}_5 e_j^* u_i^* + G_{ij}^a, \tag{B2e}$$

$$H_{ij}(\mathbf{u}^*,\mathbf{e}^*) = \mathscr{H}_1\delta_{ij} + \mathscr{H}_2 e_i^* e_j^* + \mathscr{H}_3\frac{u_i^* u_j^*}{u_s^* u_s^*} + \mathscr{H}_4 e_i^* u_j^* + \mathscr{H}_5 e_j^* u_i^* + H_{ij}^a, \tag{B2f}$$

where a_γ and g_γ for $\gamma=1,2$ and $\mathscr{A}_\gamma$, $\mathscr{B}_\gamma$, $\mathscr{G}_\gamma$, and $\mathscr{H}_\gamma$ for $\gamma=1,2,3,4,5$ are functions of $u_s^* u_s^*$ and the time varying statistics of $\mathbf{u}^*$ and $\mathbf{e}^*$. Also, a_i^a, g_i^a, A_{ij}^a, B_{ij}^a, G_{ij}^a, and H_{ij}^a are anisotropic functions of $\mathbf{u}^*$ and $\mathbf{e}^*$. The deterministic constraints are expressed via Ito calculus which applies for the Ito SDE's:

$$d(e_l^* e_l^*) = 2e_l^* de_l^* + de_l^* de_l^* = 0, \tag{B3a}$$

and

$$d(u_l^* e_l^*) = u_l^* de_l^* + e_l^* du_l^* + du_l^* de_l^* = 0. \tag{B3b}$$

The unit length of $\mathbf{e}^*$ constraint applied to the general diffusion process imposes conditions on the model:

$$e_i^* G_{ij} = e_i^* H_{ij} = 0, \tag{B4a}$$

and

$$g_i e_i^* = -\tfrac{1}{2}[G_{ij}G_{ij} + H_{ij}H_{ij}], \tag{B4b}$$

while the orthogonality constraint imposes

$$e_i^* A_{ij} + u_i^* G_{ij} = e_i^* B_{ij} + u_i^* H_{ij} = 0, \tag{B5a}$$

and

$$a_i e_i^* + g_i u_i^* = -[A_{ij}G_{ij} + B_{ij}H_{ij}]. \tag{B5b}$$

In the above conditions the independence of the Wiener processes is used to set each of their coefficients to zero.

The conditions in Eqs. (B4a) and (B5a) impose constraints on the tensorial form of the diffusion coefficients. The results for the isotropic parts are

$$A_{ij}(\mathbf{u}^*,\mathbf{e}^*) = \mathscr{A}_1\delta_{ij} + \mathscr{A}_2 e_i^* e_j^* + \mathscr{A}_3\frac{u_i^* u_j^*}{u_s^* u_s^*} - (\mathscr{G}_1 + \mathscr{G}_3)e_i^* u_j^* + \mathscr{A}_5 e_j^* u_i^* + A_{ij}^a, \tag{B6a}$$

$$B_{ij}(\mathbf{u}^*,\mathbf{e}^*) = \mathscr{B}_1\delta_{ij} + \mathscr{B}_2 e_i^* e_j^* + \mathscr{B}_3\frac{u_i^* u_j^*}{u_s^* u_s^*} - (\mathscr{H}_1 + \mathscr{H}_3)e_i^* u_j^* + \mathscr{B}_5 e_j^* u_i^* + B_{ij}^a, \tag{B6b}$$

$$G_{ij}(\mathbf{u}^*,\mathbf{e}^*) = \mathscr{G}_1(\delta_{ij} - e_i^* e_j^*) + \mathscr{G}_3\frac{u_i^* u_j^*}{u_s^* u_s^*} - (\mathscr{A}_1 + \mathscr{A}_2)\frac{u_i^* e_j^*}{u_s^* u_s^*} + G_{ij}^a, \tag{B6c}$$

$$H_{ij}(\mathbf{u}^*,\mathbf{e}^*) = \mathscr{H}_1(\delta_{ij} - e_i^* e_j^*) + \mathscr{H}_3\frac{u_i^* u_j^*}{u_s^* u_s^*} - (\mathscr{B}_1 + \mathscr{B}_2)\frac{u_i^* e_j^*}{u_s^* u_s^*} + H_{ij}^a. \tag{B6d}$$

For the anisotropic diffusion coefficients, the unit length constraint is applied without assumption, while in the orthogonality constraint each term is individually assumed to be zero. The results are conditions on the tensorial form of the anisotropic diffusion coefficients:

$$A_{ij}^a \equiv (\delta_{il} - e_i^* e_l^*)\mathscr{A}_{lj}^a, \tag{B7a}$$

$$B_{ij}^a \equiv (\delta_{il} - e_i^* e_l^*)\mathscr{B}_{lj}^a, \tag{B7b}$$

$$G_{ij}^a \equiv t_i^* t_l^* \mathscr{G}_{lj}^a, \tag{B7c}$$

$$H_{ij}^a \equiv t_i^* t_l^* \mathscr{H}_{lj}^a, \tag{B7d}$$

where a vector, $\mathbf{t}^*$, mutually orthogonal to $\mathbf{u}^*$ and $\mathbf{e}^*$ is used, and $\mathscr{A}_{lj}^a$, $\mathscr{B}_{lj}^a$, $\mathscr{G}_{lj}^a$, and $\mathscr{H}_{lj}^a$ are new anisotropic functions. From geometrical considerations a relationship between three orthogonal unit vectors exists:

$$t_i^* t_j^* = \delta_{ij} - e_i^* e_j^* - \frac{u_i^* u_j^*}{u_s^* u_s^*}. \tag{B8}$$

With the functional form of the drift coefficients substituted into Eqs. (B4b) and (B5b), expressions and conditions on the coefficients are found. Also, it is assumed that the terms consisting of the anisotropic drift coefficients are zero independent of the isotropic terms. The results are

$$g_i^a \equiv (\delta_{il} - e_i^* e_l^*)\overline{g_i^a}, \tag{B9a}$$

$$a_i^a e_i^* + \overline{g_i^a} u_i^* = 0, \tag{B9b}$$

$$\begin{aligned} a_1 = &- g_2(u_s^* u_s^*) - \{(2\mathscr{G}_1 + \mathscr{G}_3).\mathscr{A}_1 + (\mathscr{G}_1 + \mathscr{G}_3).\mathscr{A}_3 \\ &+ (\mathscr{A}_1 + \mathscr{A}_2).\mathscr{A}_5 + t_i^* t_l^*.\mathscr{A}_1 \mathscr{G}_{li}^a \\ &+ (2\mathscr{H}_1 + \mathscr{H}_3).\mathscr{B}_1 + (\mathscr{H}_1 + \mathscr{H}_3).\mathscr{B}_3 \\ &+ (\mathscr{B}_1 + \mathscr{B}_2).\mathscr{B}_5 + t_i^* t_l^*.\mathscr{B}_1 \mathscr{H}_{li}^a\}, \end{aligned} \tag{B9c}$$

and

$$\begin{aligned} g_1 = &- \mathscr{G}_1(\mathscr{G}_1 + \mathscr{G}_3) - \mathscr{H}_1(\mathscr{H}_1 + \mathscr{H}_3) - \tfrac{1}{2}(\mathscr{G}_3^2 + \mathscr{H}_3^2) \\ &- \frac{1}{2u_s^* u_s^*}[(\mathscr{A}_1 + \mathscr{A}_2)^2 + (\mathscr{B}_1 + \mathscr{B}_2)^2] \\ &- \tfrac{1}{2} t_i^* t_l^* (\mathscr{G}_1 \mathscr{G}_{li}^a + \mathscr{H}_1 \mathscr{H}_{li}^a). \end{aligned} \tag{B9d}$$

The constraint of a joint normal solution in isotropic, decaying turbulence is applied by comparison with the Langevin equation whose solution for the PDF is known to be joint normal. The actual comparison is made between the SDE's for speed from the different equations. The Langevin equation is

$$du_i = -a u_i dt + b dW_i, \tag{B10}$$

which when expressed for the speed, $u \equiv |\mathbf{u}|$, is

$$du = \left(\frac{b^2}{u} - au\right) dt + b dW. \tag{B11}$$

In isotropic turbulence the SDE for speed from the general model with the stochastic constraints applied is

$$du = E_1 dt + E_2 dW, \tag{B12a}$$

where

$$\begin{aligned} E_1 = &[\mathscr{A}_1(\mathscr{A}_1 + \mathscr{A}_2) + \mathscr{B}_1(\mathscr{B}_1 + \mathscr{B}_2) + \tfrac{1}{2}(\mathscr{A}_2^2 + \mathscr{B}_2^2)]\frac{1}{u} \\ &+ [a_2 + \tfrac{1}{2}(\mathscr{G}_1 + \mathscr{G}_3)^2 + \tfrac{1}{2}(\mathscr{H}_1 + \mathscr{H}_3)^2]u, \end{aligned} \tag{B12b}$$

$$E_2 = [(\mathscr{A}_1 + \mathscr{A}_3)^2 + (\mathscr{B}_1 + \mathscr{B}_3)^2 + (\mathscr{A}_5^2 + \mathscr{B}_5^2)u^2]^{1/2}. \tag{B12c}$$

This equation must be forced into the form of Eq. (B11). A fully general model would consist of diffusion coefficients which are power or Laurent series in $\mathbf{u}$, but to avoid this complexity the coefficients are assumed independent of u where possible. Thus, by scaling with ε and k all the coefficients are re-expressed with non-dimensional parameters and the appropriate u dependencies where necessary:

$$a_i^a \equiv \tilde{a}_i^a\left(\frac{\varepsilon}{\sqrt{k}}\right), \quad a_1 \equiv \tilde{a}_1\left(\frac{\varepsilon}{\sqrt{k}}\right), \quad a_2 \equiv \tilde{a}_2^{(1)}\left(\frac{\varepsilon}{k}\right) + \tilde{a}_2^{(2)}\left(\frac{2\varepsilon}{u^2}\right),$$

$$\overline{g_i^a} \equiv \tilde{g}_i^a\left(\frac{\varepsilon}{k}\right), \quad g_1 \equiv \tilde{g}_1\left(\frac{\varepsilon}{k}\right), \quad g_2 \equiv \tilde{g}_2 \frac{\varepsilon}{\sqrt{k^3}},$$

$$\mathscr{A}_1 \equiv \tilde{\mathscr{A}}_1\sqrt{\varepsilon}, \quad \mathscr{A}_2 \equiv \tilde{\mathscr{A}}_2\sqrt{\varepsilon}, \quad \mathscr{A}_3 \equiv \tilde{\mathscr{A}}_3\sqrt{\varepsilon}, \quad \mathscr{A}_5 \equiv \tilde{\mathscr{A}}_5\frac{\sqrt{2\varepsilon}}{u}, \quad \mathscr{A}_{lj}^a \equiv \tilde{\mathscr{A}}_{lj}^a\sqrt{\varepsilon},$$

$$\mathscr{B}_1 \equiv \tilde{\mathscr{B}}_1\sqrt{\varepsilon}, \quad \mathscr{B}_2 \equiv \tilde{\mathscr{B}}_2\sqrt{\varepsilon}, \quad \mathscr{B}_3 \equiv \tilde{\mathscr{B}}_3\sqrt{\varepsilon}, \quad \mathscr{B}_5 \equiv \tilde{\mathscr{B}}_5\frac{\sqrt{2\varepsilon}}{u}, \quad \mathscr{B}_{lj}^a \equiv \tilde{\mathscr{B}}_{lj}^a\sqrt{\varepsilon},$$

$$\mathscr{G}_1 \equiv \tilde{\mathscr{G}}_1\sqrt{\frac{\varepsilon}{k}}, \quad \mathscr{G}_3 \equiv \tilde{\mathscr{G}}_3\sqrt{\frac{\varepsilon}{k}}, \quad \mathscr{G}_{lj}^a \equiv \tilde{\mathscr{G}}_{lj}^a\sqrt{\frac{\varepsilon}{k}},$$

$$\mathscr{H}_1 \equiv \tilde{\mathscr{H}}_1\sqrt{\frac{\varepsilon}{k}}, \quad \mathscr{H}_3 \equiv \tilde{\mathscr{H}}_3\sqrt{\frac{\varepsilon}{k}}, \quad \mathscr{H}_{lj}^a \equiv \tilde{\mathscr{H}}_{lj}^a\sqrt{\frac{\varepsilon}{k}},$$

The joint normal condition is now applied giving an expression for one of the velocity drift coefficients:

$$\begin{aligned} \tilde{a}_2^{(2)} = &\tfrac{1}{2}\{.\tilde{\mathscr{A}}_3(2.\tilde{\mathscr{A}}_1 + \tilde{\mathscr{A}}_3) - \tfrac{1}{2}\tilde{\mathscr{A}}_2(2.\tilde{\mathscr{A}}_1 + \tilde{\mathscr{A}}_2) + 2.\tilde{\mathscr{A}}_5^2 + \tilde{\mathscr{B}}_3(2.\tilde{\mathscr{B}}_1 + \tilde{\mathscr{B}}_3) - \tfrac{1}{2}\tilde{\mathscr{B}}_2(2.\tilde{\mathscr{B}}_1 + \tilde{\mathscr{B}}_2) + 2.\tilde{\mathscr{B}}_5^2. \end{aligned} \tag{B13}$$

The evolution of the kinetic energy constraint is applied by forcing the kinetic energy equation from the stochastic model into the same form as Eq. (51), which results in an expression for the remaining velocity drift coefficient:

$$\tilde{a}_2^{(1)} = -\frac{1}{2}\Bigg\{ 1 + \frac{1}{\sqrt{k}}\langle u_l^* \tilde{a}_l^a \rangle + (\tilde{\mathscr{G}}_1 + \tilde{\mathscr{G}}_3)^2 + (\tilde{\mathscr{H}}_1 + \tilde{\mathscr{H}}_3)^2 + \tfrac{3}{2}(\tilde{\mathscr{A}}_1 + \tilde{\mathscr{A}}_3)^2 + 3.\tilde{\mathscr{A}}_5^2 + \tilde{\mathscr{A}}_1 \langle (\delta_{jl} - e_j^* e_l^*).\tilde{\mathscr{A}}_{lj}^a \rangle + \tilde{\mathscr{A}}_3 \left\langle \frac{u_j^* u_l^*}{u_s^* u_s^*}.\tilde{\mathscr{A}}_{lj}^a \right\rangle$$

$$+ \sqrt{2}.\tilde{\mathscr{A}}_5 \left\langle \frac{e_j^* u_l^*}{(u_s^* u_s^*)^{1/2}}.\tilde{\mathscr{A}}_{lj}^a \right\rangle + \tfrac{1}{2}\langle (\delta_{ln} - e_l^* e_n^*).\tilde{\mathscr{A}}_{lj}^a.\tilde{\mathscr{A}}_{nj}^a \rangle + \tfrac{3}{2}(\tilde{\mathscr{B}}_1 + \tilde{\mathscr{B}}_3)^2 + 3.\tilde{\mathscr{B}}_5^2 + \tilde{\mathscr{B}}_1 \langle (\delta_{jl} - e_j^* e_l^*).\tilde{\mathscr{B}}_{lj}^a \rangle$$

$$+ \tilde{\mathscr{B}}_3 \left\langle \frac{u_j^* u_l^*}{u_s^* u_s^*}.\tilde{\mathscr{B}}_{lj}^a \right\rangle + \sqrt{2}.\tilde{\mathscr{B}}_5 \left\langle \frac{e_j^* u_l^*}{(u_s^* u_s^*)^{1/2}}.\tilde{\mathscr{B}}_{lj}^a \right\rangle + \tfrac{1}{2}\langle (\delta_{ln} - e_l^* e_n^*).\tilde{\mathscr{B}}_{lj}^a.\tilde{\mathscr{B}}_{nj}^a \rangle. \tag{B14}$$

The final form for the General **u**-**e** Model is now summarized:

$$du_i^* = \left(\frac{\varepsilon}{k}\right)\Bigg[\tilde{a}_1 \sqrt{k} e_i^* + \tilde{a}_2^{(1)} u_i^* + 2\tilde{a}_2^{(2)} \frac{k}{u_s^* u_s^*} u_i^* + \tilde{a}_i^a \sqrt{k} \Bigg] dt + A_{ij} dW_j + B_{ij} dW_j', \tag{B15a}$$

and

$$de_i^* = \left(\frac{\varepsilon}{k}\right)\left[\tilde{g}_1 e_i^* + \tilde{g}_2 \frac{u_i^*}{\sqrt{k}} + (\delta_{ij} - e_i^* e_j^*)\tilde{g}_j^a \right] dt + G_{ij} dW_j + H_{ij} dW_j', \tag{B15b}$$

where some of the coefficients were previously given in Eqs. (B13) and (B14), and the following coefficients are re-expressed in non-dimensional form:

$$\tilde{a}_1 = -\tilde{g}_2 \frac{u_s^* u_s^*}{k} - \{ (2.\tilde{\mathscr{G}}_1 + \tilde{\mathscr{G}}_3).\tilde{\mathscr{A}}_1 + (\tilde{\mathscr{G}}_1 + \tilde{\mathscr{G}}_3).\tilde{\mathscr{A}}_3 + (\tilde{\mathscr{A}}_1 + \tilde{\mathscr{A}}_2).\tilde{\mathscr{A}}_5 + t_i^* t_l^*.\tilde{\mathscr{A}}_1 \tilde{\mathscr{G}}_{li}^a + (2.\tilde{\mathscr{H}}_1 + \tilde{\mathscr{H}}_3).\tilde{\mathscr{B}}_1 + (\tilde{\mathscr{H}}_1 + \tilde{\mathscr{H}}_3).\tilde{\mathscr{B}}_3 + (\tilde{\mathscr{B}}_1 + \tilde{\mathscr{B}}_2).\tilde{\mathscr{B}}_5 + t_i^* t_l^*.\tilde{\mathscr{B}}_1 \tilde{\mathscr{H}}_{li}^a \}, \tag{B16a}$$

$$\tilde{g}_1 = -\tilde{\mathscr{G}}_1(\tilde{\mathscr{G}}_1 + \tilde{\mathscr{G}}_3) - \tilde{\mathscr{H}}_1(\tilde{\mathscr{H}}_1 + \tilde{\mathscr{H}}_3) - \tfrac{1}{2}(\tilde{\mathscr{G}}_3^2 + \tilde{\mathscr{H}}_3^2) - \frac{k}{2u_s^* u_s^*}[(\tilde{\mathscr{A}}_1 + \tilde{\mathscr{A}}_2)^2 + (\tilde{\mathscr{B}}_1 + \tilde{\mathscr{B}}_2)^2] - \tfrac{1}{2} t_i^* t_l^* (\tilde{\mathscr{G}}_1 \tilde{\mathscr{G}}_{li}^a + \tilde{\mathscr{H}}_1 \tilde{\mathscr{B}}_{li}), \tag{B16b}$$

$$A_{ij}(\mathbf{u}^*, \mathbf{e}^*) = \sqrt{\varepsilon}\Bigg[\tilde{\mathscr{A}}_1 \delta_{ij} + \tilde{\mathscr{A}}_2 e_i^* e_j^* + \tilde{\mathscr{A}}_3 \frac{u_i^* u_j^*}{u_s^* u_s^*} - \frac{1}{\sqrt{k}}(\tilde{\mathscr{G}}_1 + \tilde{\mathscr{G}}_3) e_i^* u_j^* + \sqrt{2}.\tilde{\mathscr{A}}_5 \frac{e_j^* u_i^*}{(u_s^* u_s^*)^{1/2}} + (\delta_{il} - e_i^* e_l^*)\tilde{A}_{lj}^a \Bigg], \tag{B16c}$$

$$B_{ij}(\mathbf{u}^*, \mathbf{e}^*) = \sqrt{\varepsilon}\Bigg[\tilde{\mathscr{B}}_1 \delta_{ij} + \tilde{\mathscr{B}}_2 e_i^* e_j^* + \tilde{\mathscr{B}}_3 \frac{u_i^* u_j^*}{u_s^* u_s^*} - \frac{1}{\sqrt{k}}(\tilde{\mathscr{H}}_1 + \tilde{\mathscr{H}}_3) e_i^* u_j^* + \sqrt{2}.\tilde{\mathscr{B}}_5 \frac{e_j^* u_i^*}{(u_s^* u_s^*)^{1/2}} + (\delta_{il} - e_i^* e_l^*)\tilde{B}_{lj}^a \Bigg], \tag{B16d}$$

$$G_{ij}(\mathbf{u}^*, \mathbf{e}^*) = \sqrt{\frac{\varepsilon}{k}}\Bigg[\tilde{\mathscr{G}}_1(\delta_{ij} - e_i^* e_j^*) + \tilde{\mathscr{G}}_3 \frac{u_i^* u_j^*}{u_s^* u_s^*} - \sqrt{k}(\tilde{\mathscr{A}}_1 + \tilde{\mathscr{A}}_2)\frac{u_i^* e_j^*}{u_s^* u_s^*} + t_i^* t_l^* \tilde{G}_{lj}^a \Bigg], \tag{B16e}$$

$$H_{ij}(\mathbf{u}^*, \mathbf{e}^*) = \sqrt{\frac{\varepsilon}{k}}\Bigg[\tilde{\mathscr{H}}_1(\delta_{ij} - e_i^* e_j^*) + \tilde{\mathscr{H}}_3 \frac{u_i^* u_j^*}{u_s^* u_s^*} - \sqrt{k}(\tilde{\mathscr{B}}_1 + \tilde{\mathscr{B}}_2)\frac{u_i^* e_j^*}{u_s^* u_s^*} + t_i^* t_l^* \tilde{H}_{ij}^a \Bigg]. \tag{B16f}$$

In addition, one constraint remains on the anisotropic drift terms:

$$\sqrt{k}\tilde{a}_l^a e_l^* + \tilde{g}_l^a u_l^* = 0. \tag{B17}$$

[1] P. Y. Chou, ''On velocity correlations and the solutions of the equations of turbulent fluctuation,'' Q. Appl. Math. **3**, 38 (1945).
[2] J. Rotta, ''Statistische theorie nichthomogener turbulenz,'' Z. Phys. **129**, 547 (1951).
[3] B. E. Launder, G. J. Reece, and W. Rodi, ''Progress in the development of a Reynolds-stress turbulence closure,'' J. Fluid Mech. **68**, 537 (1975).
[4] T. H. Shih and J. L. Lumley, ''Modeling of pressure correlation terms in Reynolds stress and scalar flux equations,'' Technical Report FDA-85-3, Cornell University, 1985.
[5] D. C. Haworth and S. B. Pope, ''A generalized Langevin model for turbulent flows,'' Phys. Fluids **29**, 387 (1986).
[6] S. Fu, B. E. Launder, and D. P. Tselepidakis, ''Accommodating the effects of high strain rates in modelling the pressure-strain correlation,'' Technical Report TFD/87/5, UMIST Mech. Eng. Dept. Report TFD/89/1, 1987.
[7] C. G. Speziale, S. Sarkar, and T. B. Gatski, ''Modelling the pressure-strain correlation of turbulence: an invariant dynamical systems approach,'' J. Fluid Mech. **227**, 245 (1991).
[8] A. V. Johansson and M. Hällback, ''Modelling of rapid pressure-strain in Reynolds-stress closures,'' J. Fluid Mech. **269**, 143 (1994).
[9] J. R. Ristorcelli, J. L. Lumley, and R. Abid, ''A rapid-pressure covariance representation consistent with the Taylor-Proudman theorem materially indifferent in the two-dimensional limit,'' J. Fluid Mech. **292**, 111 (1995).

[10]J. L. Lumley and G. R. Newman, ''The return to isotropy of homogeneous turbulence,'' J. Fluid Mech. **82**, 161 (1977).
[11]S. Sarkar and C. G. Speziale, ''A simple nonlinear model for the return to isotropy in turbulence,'' Phys. Fluids A **2**, 84 (1990).
[12]M. K. Chung and S. K. Kim, ''A nonlinear return-to-isotropy model with Reynolds number and anisotropy dependency,'' Phys. Fluids A **7**, 1425 (1995).
[13]W. C. Reynolds, ''Effects of rotation on homogeneous turbulence,'' in *Proceedings of the Tenth Australasian Fluid Mechanics Conference*, 1989.
[14]C. Cambon and L. Jacquin, ''Spectral approach to non-isotropic turbulence subjected to rotation,'' J. Fluid Mech. **202**, 295 (1989).
[15]N. N. Mansour, T. H. Shih, and W. C. Reynolds, ''The effects of rotation on initially anisotropic homogeneous flows,'' Phys. Fluids A **3**, 2421 (1991).
[16]W. C. Reynolds and S. C. Kassinos, ''A one-point model for the evolution of the Reynolds stress and structure tensors in rapidly deformed homogeneous turbulence,'' Proc. R. Soc. London A 451 (1941), 87 (1995).
[17]C. G. Speziale, R. Abid, and G. A. Blaisdell, ''On the consistency of Reynolds stress turbulence closures with hydrodynamic stability theory,'' Phys. Fluids A **8**, 781 (1996).
[18]L. Prandtl, in NACA Technical Memo, 1933.
[19]G. I. Taylor, ''Turbulence in a contracting stream,'' Z. Angew Math. Mech. **15**, 91 (1935).
[20]G. K. Batchelor and I. Proudman, ''The effect of rapid distortion of a fluid in turbulent motion,'' Q. J. Mech. Appl. Math. **7**, 83 (1954).
[21]A. A. Townsend, *The Structure of Turbulent Shear Flow*, 2nd ed. (Cambridge University Press, Cambridge, 1976).
[22]M. J. Lee and W. C. Reynolds, ''Numerical experiments on the structure of homogeneous turbulence,'' Technical Report TF-24, Stanford University, November 1985.
[23]M. J. Lee, ''Distortion of homogeneous turbulence by axisymmetric strain and dilatation,'' Phys. Fluids A **1**, 1541 (1989).
[24]M. J. Lee, J. Kim, and P. Moin, ''Structure of turbulence at high shear rate,'' J. Fluid Mech. **216**, 561 (1990).
[25]J. C. R. Hunt and D. J. Carruthers, ''Rapid distortion theory and the 'problems' of turbulence,'' J. Fluid Mech. **212**, 497 (1990).
[26]S. C. Kassinos and W. C. Reynolds, ''A structure-based model for rapid distortion of homogeneous turbulence,'' Technical Report TF-61, Stanford University, 1994.
[27]S. C. Kassinos and W. C. Reynolds, ''An extended structure-based model based on a stochastic eddy-axis evolution equation,'' *Annual Research Briefs*: *Center for Turbulence Research* (1995), pp. 133–148.
[28]S. C. Kassinos and W. C. Reynolds (private communication, April 1996).
[29]S. B. Pope, ''Pdf methods for turbulent reactive flows,'' Prog. Energy Combust. Sci. **11**, 119 (1985).
[30]S. B. Pope and Y. L. Chen, ''The velocity-dissipation probability density function model for turbulent flows,'' Phys. Fluids A **2**, 1437 (1990).
[31]S. B. Pope, ''Application of the velocity-dissipation probability density function model to inhomogeneous turbulent flows,'' Phys. Fluids A **3**, 1947 (1991).
[32]S. B. Pope, ''Lagrangian pdf methods for turbulent flows,'' Annu. Rev. Fluid Mech. **26**, 23 (1994).
[33]S. B. Pope, ''On the relationship between stochastic Lagrangian models of turbulence and second-moment closures,'' Phys. Fluids A **6**, 973 (1994).
[34]P. A. Durbin and C. G. Speziale, ''Realizability of second-moment closure via stochastic analysis,'' J. Fluid Mech. **280**, 395 (1994).
[35]H. A. Wouters, T. W. J. Peeters, and D. Roekaerts, ''On the existence of a stochastic Lagrangian model representation for second-moment closures,'' Phys. Fluids A **8**, 1702 (1996).
[36]G. K. Batchelor, *The Theory of Homogeneous Turbulence* (Cambridge University Press, Cambridge, 1953).
[37]R. S. Rogallo, ''Numerical experiments in homogeneous turbulence,'' Technical Report 81315, NASA, 1981.
[38]A. Craya, ''Contribution à l'analyse de la turbulence associée à des vitesses moyennes,'' 1958. P.S.T. no. 345.
[39]Z. Warhaft, ''An experimental study of the effect of uniform strain on thermal fluctuations in grid-generated turbulence,'' J. Fluid Mech. **99**, (1980).
[40]K. S. Choi and J. L. Lumley, ''Return to isotropy of homogeneous turbulence revisited,'' in *Turbulence and Chaotic Phenomena in Fluids*, edited by T. Tatsumi (Elsevier, New York, 1984), pp. 267–272.
[41]K. Hanjalić and B. E. Launder, ''A Reynolds stress model of turbulence and its applications,'' J. Fluid Mech. **52**, 609 (1972).
[42]M. M Rogers, P. Moin, and W. C. Reynolds, ''The structure and modeling of the hydrodynamic and passive scalar fields in homogeneous turbulent shear flow,'' Technical Report TF-25, Stanford University, August 1986.
[43]S. Tavoularis and U. Karnik, ''Further experiments on the evolution of turbulent stresses and scales in uniformly sheared turbulence,'' J. Fluid Mech. **204**, 457 (1989).
[44]J. Bardina, J. H. Fersiger, and W.C. Reynolds, ''Improved turbulence models based on large-eddy simulation of homogeneous, incompressible turbulent flows,'' Technical Report TF-19, Stanford University, 1983.
[45]C. G. Speziale and N. Mac Giolla Mhuiris, ''On the prediction of equilibrium states in homogeneous turbulence,'' J. Fluid Mech. **209**, 591 (1989).
[46]H. J. Tucker, Ph.D. thesis, McGill University, Montreal, 1970.
[47]G. A. Blaisdell and K. Shariff, ''Homogeneous turbulence subjected to mean flow with elliptic stream lines,'' in *Studying Turbulence Using Numerical Simulation Databases - V*, December 1994. Center for Turbulence Research: Proceedings of the Summer Program 1994.
[48]C. Cambon, C. Teissèdre, and D. Jeandel, ''Etude d'éffets couplés de déformation et de rotation sur une turbulence homogéne,'' J. Méc. Theoéo. Appl. **4**, 629 (1985).
[49]R. T. Pierrehumbert, ''Universal short-wave instability of two-dimensional eddies in an inviscid fluid,'' Phys. Rev. Lett. **57**, 2157 (1986).
[50]B. J. Bayly, ''Three-dimensional instability of ellipitical flow,'' Phys. Rev. Lett. **57**, 2160 (1986).
[51]M. J. Landman and P. G. Saffman, ''The three-dimensional instability of strained vortices in a viscous fluid,'' Phys. Fluids **30**, 2339 (1987).
[52]F. Waleffe, ''The three-dimensional instability of strained vortices,'' Phys. Fluids A **2**, 76 (1990).